
Intermediate ocean circulation and cryosphere dynamics in the northeast Atlantic during Heinrich Stadials: benthic foraminiferal assemblage response

Depuydt Pauline ^{1,*}, Mojtahid Meryem ¹, Barras Christine ¹, Bouhdayad Fatima Zohra ¹, Toucanne Samuel ²

¹ Univ Angers, Nantes Université, Le Mans Université, CNRS, UMR 6112, Laboratoire de Planétologie et Géosciences, F-49000, Angers, France

² Univ Brest, CNRS, Ifremer, Geo-Ocean, F-29280, Plouzane, France

* Corresponding author : Pauline Depuydt, email address : pauline.depuydt@univ-angers.fr

Abstract :

The interaction between ocean circulation and ice-sheet dynamics plays a key role in the Quaternary climate. Compared with the surface and deep regions of the Atlantic Meridional Overturning Circulation (AMOC), the study of intermediate depths during key time periods, such as Heinrich Stadials (HSs), remains poorly documented, especially for the northeast Atlantic. Here we use benthic foraminiferal assemblage data to trace palaeoenvironmental changes from similar to 32 to 14 ka cal BP at similar to 1000 m depth in the Bay of Biscay. Our results highlight the high sensitivity of foraminifera, with species-specific responses, to continental (European Ice Sheet dynamics) and marine (AMOC) forcing factors during the last three HSs. In general, HSs were characterised by the concomitant presence of meso-oligotrophic and anoxia indicator species and the low abundance of high-energy indicator species. This confirms an overall sluggish intermediate circulation during the three HSs in the northeast Atlantic. HS1 is distinctive for its abundance of high-organic flux indicator species during its early phase. This is consistent with the fact that HS1 was by far the most important period of ice-sheet retreat and meltwater release into the ocean over the studied time interval. Finally, foraminifera depict the mid-HS2 reventilation event due to regional glacier instabilities.

Keywords : AMOC, benthic foraminifera, Channel River, European Ice Sheet, Glacial Eastern Boundary Current (GEBC), intermediate water masses

41 **1. Introduction**

42 The last glacial-interglacial cycle is a critical period to understand the natural climate
43 variability and its abrupt transitions (e.g. Bond *et al.*, 1993; Wang *et al.*, 2001; Clark *et al.*,
44 2012; Denton *et al.*, 2021). Orbital forcing (solar radiation), and the feedbacks implying the
45 atmosphere, the ocean, and the cryosphere are the main factors explaining the recorded
46 centennial to multi-millennial climate variability over this period (Broecker and Denton, 1990;
47 McManus *et al.*, 1999; Denton *et al.*, 2010; Lynch-Stieglitz, 2017). In the Northern Hemisphere,
48 the climate of the last glacial period was punctuated by cold (stadials) and warm intervals
49 (interstadials), that were coeval with periods of weakened and accelerated Atlantic Meridional
50 Overturning Circulation (AMOC), respectively (e.g. Kissel *et al.*, 2008; Böhm *et al.*, 2015;
51 Henry *et al.*, 2016; Toucanne *et al.*, 2021). Amongst the cold intervals, the most drastic are
52 certainly the Heinrich Stadials (HSs), encompassing the Heinrich events (HEs), i.e. armadas of
53 icebergs discharge issued from the dislocation of the Hudson Strait Ice stream of the Laurentide
54 Ice Sheet (LIS) that ultimately caused the deposition of ice-rafted debris (IRD) rich sediments
55 in the subpolar North Atlantic (Hemming, 2004). It is hypothesized that HEs were triggered by
56 sub-surface heat (700–1100 m depth), 1-2 ka after the decline of the AMOC (Shaffer *et al.*,
57 2004; Marcott *et al.*, 2011; Alvarez-Solas *et al.*, 2013). The initial AMOC slowdown likely
58 requires precursor melting of North Atlantic–adjacent ice sheets and it is now accepted that the
59 European Ice sheet (EIS) was a critical source for AMOC destabilization and the initiation of
60 HSs conditions (Peck *et al.*, 2006; Eynaud *et al.*, 2012; Boswell *et al.*, 2019; Toucanne *et al.*,
61 2015, 2021, 2022).

62 The present work investigates the evolution of northeast Atlantic intermediate water depth
63 environments and their interaction with EIS dynamics during the last glacial and deglaciation
64 periods, with a focus on HSs. This is achieved through the study of marine sediment core
65 BOBGEO-CS05 retrieved at ~1000 m water depth in the northern Bay of Biscay (BoB) (Fig. 1a
66 & 1c). This record covers the past ~32-14 ka cal BP, thus encompassing the last three HSs
67 (HS1, HS2 and HS3). During the last glacial period and the last deglaciation, BOBGEO-CS05
68 site was located off the Channel River, that drained EIS sediment-laden meltwaters to the
69 northern BoB (Zaragosi *et al.*, 2001; Bourillet and Lericolais, 2003; Toucanne *et al.*, 2009,
70 2010) (Fig. 1b). At the time, the core site was also on the pathway of the Glacial Eastern
71 Boundary Current (GEBC), the glacial analogue of the northward-flowing European Slope
72 Current, that represents the easternmost portion of the upper branch of the AMOC (Toucanne

73 *et al.*, 2021) (Fig. 1b). As such, core BOBGEO-CS05 is ideally located to track EIS melting
74 episodes and evaluate their impact/relation to the upper branch of the AMOC.

75 The present study focuses on fossil benthic foraminifera as one of the very few biological
76 indicator groups that are able to record the history of events on the seafloor by integrating the
77 cumulative impacts of the changing physico-chemical habitats (e.g. Schmiedl and Mackensen,
78 1997; Wollenburg *et al.*, 2001; Rodriguez-Lazaro *et al.*, 2017). A particular interest is found in
79 documenting HS2 and HS3, which are not covered by the nearby recent foraminiferal studies
80 (Mojtahid *et al.*, 2017; Pascual *et al.*, 2020). In addition, our aim is to establish to what extent
81 information previously obtained from sedimentary, geochemical and surface water proxies on
82 the interaction between the AMOC and the EIS during the HSs are consistent with our benthic
83 biotic data. More specifically, the approach uses here foraminiferal diversity and density, and
84 the ecological requirements of specific species to interpret several aspects of the environment
85 on the seafloor (e.g. organic matter flux, bottom-water oxygenation, current, transport, water
86 masses properties). Our findings highlight strong foraminiferal species-specific responses,
87 particularly during HSs, with some species associations able to discriminate between
88 EIS/continental impact and ocean circulation changes.

89

90 **2. Core location, present and past sedimentological and hydrographical settings**

91 Core BOBGEO-CS05 (46°18.850'N, 5°56.988'W, 1473 cm length, 1015 m water depth) was
92 extracted from the upper continental slope of the northern BoB (northeast Atlantic) during the
93 BOBGEO cruise (doi.org/10.17600/9030060; R/V Pourquoi pas?; Bourillet, 2009) (Fig. 1).
94 Core BOBGEO-SC05 is mostly composed of contourite deposits (Toucanne *et al.*, 2021), i.e.
95 sediments deposited or substantially reworked by the persistent action (e.g. selective deposition,
96 winnowing, erosion) of bottom currents (Facies 1 and 2; Fig. 2). Silty-clayey laminations
97 characterized the early part of the deglaciation (early HS1), ca. 18-16.7 ka (Facies 3; Fig. 2),
98 and IRD (Facies 4; Fig. 2) allowed the recognition of the Heinrich layers (cf. Supplementary
99 material S1 for the complete X-Ray radiographs).

100 Today, the sedimentation on the slope is governed by the European Slope Current
101 (ESC), flowing along the upper slope (~500-2000 m water depth) from the northern Iberian
102 Peninsula to the Faroe-Shetland Channel (Marsh *et al.*, 2017; Clark *et al.*, 2021; Moritz *et al.*,
103 2021) (Fig. 1a). This current, driven by both the steep topography of the European margin and
104 large-scale meridional density gradients (Huthnance, 1984; Pingree and Cann, 1990; Friocourt

105 *et al.*, 2007), is largely recruited from the eastern North Atlantic and is connected, north of
106 $\sim 55^\circ\text{N}$ (i.e. Rockall Trough), to the upper part of the North Atlantic Current (NAC; that is the
107 eastern limb of the subpolar gyre). This forms the bulk of the upper branch of the AMOC (down
108 to ~ 1500 m; Lozier *et al.*, 2019; Huthnance *et al.*, 2020). The latter (to which the ESC
109 contributes by $\sim 25\%$; Berx *et al.*, 2013) finally reaches the Nordic Seas convection region,
110 where it cools and sinks to form a deeper southward return flow, the North Atlantic Deep Water
111 (NADW), mainly found along the eastern continental margin of North America and transported
112 by the Deep Western Boundary Current (e.g. Dickson and Brown, 1994) (Fig. 1a).

113 The main water mass transported by the NAC into the BoB forms the Eastern North Atlantic
114 Central Water (ENACW), found down to ~ 600 m water depth (Pollard and Pu, 1985). Below,
115 the Mediterranean Outflow Water (MOW) is present between ~ 600 and 1500 m, flowing
116 northward from the Gulf of Cadiz and largely entrained by the ESC north of $\sim 45^\circ\text{N}$ (e.g. Pingree
117 *et al.*, 1999; van Aken, 2000). Deeper, the Labrador Sea Water (LSW), centered at ~ 2000 m
118 water depth and corresponding to the upper NADW, dominates (van Aken, 2000). The upper
119 NADW in the eastern North Atlantic and the BoB reflects recirculation processes, i.e. capture
120 of the (southward-flowing) LSW by the above (eastward-flowing) Gulf Stream – NAC system
121 in the north-western North Atlantic (Buckley and Marshall, 2016; Zou *et al.*, 2017) (Fig. 1a).

122 During the last glacial maximum (LGM) ca. 23-18 ka cal BP (Mix *et al.*, 2001), the Gulf
123 Stream – NAC system and more generally the upper branch of the AMOC certainly had a
124 different geometry (i.e. positioned southward) because of the (southward) expansion of ice
125 sheets over North America (Keffer *et al.*, 1988; Otto-Bliesner *et al.*, 2006; Brady and Otto-
126 Bliesner, 2011; Löffverström *et al.*, 2014) (Fig. 1b). The NADW was likely replaced by a
127 shallower, northern-sourced nutrient-poor water mass, namely the Glacial North Atlantic
128 Intermediate Water (GNAIW), dominant above 2000 m depth and overlaying a more nutrient-
129 rich water of southern origin below 2000 m (i.e. a glacial analog of Antarctic Bottom Water)
130 (e.g. Lynch-Stieglitz *et al.*, 2007). The recirculation of the GNAIW by the glacial Gulf Stream
131 – NAC system certainly explains GNAIW signatures recorded in the NE Atlantic basin and the
132 BoB basin during the last glacial period (Zahn *et al.*, 1997; Peck *et al.*, 2006, 2007; Toucanne
133 *et al.*, 2021). At the same time, the Mediterranean-Atlantic water exchange was reduced by
134 $\sim 50\%$, and the MOW was certainly restricted to the southern Iberian margin (e.g. Rogerson *et al.*
135 *et al.*, 2012). On the other hand, the presence of Antarctic Intermediate waters (AAIW) along the
136 European margin as far north as the South Iceland Rise was hypothesized (Rickaby and
137 Elderfield, 2005; Thornalley *et al.*, 2010) but the recent studies of Thornalley *et al.* (2015) then

138 Crocker *et al.* (2016) concluded that mid-depth in the NE Atlantic was never ventilated by
139 southern-sourced waters during the last glacial period. During late HS1 (~17 ka), and the near
140 shutdown of the AMOC (McManus *et al.*, 2004; Ng *et al.*, 2018), Mojtahid *et al.* (2017)
141 recorded low foraminiferal Sr/Ca ratios (i.e. carbonate system proxy; Yu *et al.*, 2014; Allen *et*
142 *al.*, 2016; Keul *et al.*, 2017), indicative of a change in water mass chemistry and origin in the
143 BoB. At the same time, Mojtahid *et al.* (2017) recorded increasing benthic foraminiferal Mg/Ca
144 ratios, indicating a warming of intermediate water masses. This is interpreted as the northward
145 conveyance of the subsurface warming originating from the low latitudes (Rühlemann *et al.*,
146 2004; Shaffer *et al.*, 2004) by the glacial NAC (GNAC) and the GEBC (Fig. 1b) (Toucanne *et*
147 *al.*, 2021). This reinforces the view that the water mass structure in the glacial NE Atlantic
148 could have changed rapidly through time.

149

150 **3. Materials and Methods**

151 **3.1. Chronology**

152 The chronostratigraphic framework of core BOBGEO-CS05 (Fig. 2) is detailed in Toucanne *et*
153 *al.* (2021). In short, the final age model is based on XRF-Ca/Ti data synchronization with the
154 nearby well-dated core MD95-2002 (Fig. 2a). Twenty-one XRF tie-points based on the
155 recognition of millennial-scale oscillations were determined. The final age model indicates that
156 core BOBGEO-CS05 covers a period extending from ca. 32 to 14 ka cal BP (Fig. 2), thus
157 encompassing the end of MIS 3 (ca. 57-29 ka cal BP) and MIS 2 (ca. 29-14.7 ka cal BP). The
158 accuracy of the age model is supported first by the good match between the percentages of the
159 polar planktonic taxon *N. pachyderma* in core BOBGEO-CS05 and MD95-2002 (Fig. 2c), and
160 second, by the overall concordance with the new radiocarbon dates (n=12; Table 1; Fig. 2b).
161 The top core ¹⁴C dates show older ages (~15.7 cal ka BP) than the final XRF-Ca/Ti based age
162 model (~14 cal ka BP) (Fig. 2b). The low percentages of the polar taxon *N. pachyderma* at the
163 core top (Fig. 2c) indicate that we are out of the Heinrich Stadial, making the core top ¹⁴C ages
164 unreliable. Such incoherencies in ¹⁴C dates (including the few outliers; Fig. 2b) are certainly
165 linked to physical sediment mixing and bioturbation that are common in contourite deposits.

166 The final age model clearly shows a sedimentary hiatus after ~14 cal ka BP, in concordance
167 with previous studies in similar environments in the BoB (Mojtahid *et al.*, 2017; Toucanne *et*
168 *al.*, 2021). The lack of sedimentation is due to increased erosion of the shelf deposits in response

169 to the significant sea-level rise and the embayment of the English Channel (e.g., Bourillet *et al.*,
170 2003; Toucanne *et al.*, 2012).

171 Core BOBGEO-CS05 shows sedimentation rates of 50-150 cm.ka⁻¹ (Fig. 2b). As such, core
172 BOBGEO-CS05 offers a unique opportunity to study at high time resolution the later part of
173 the last glacial period and the last three HSs.

174

175 **3.2. Foraminiferal analyses**

176 For benthic foraminiferal analyses, 56 samples were investigated (~320 years resolution). The
177 samples were washed through 63 and 150 µm mesh size sieves. The >150 µm fraction was
178 splitted with a dry Otto microsplitter (when necessary) until obtaining at least 250-300
179 specimens in the final split. Then, all foraminifera were picked out from the split and mounted
180 on Plummer cell slides for taxonomic determination. To verify the relevance of small-sized
181 benthic species, 16 out of the 56 samples were investigated from the 63-150 µm size fraction.
182 Foraminifera were picked out from 3 out of the 16 samples, put in Plummer cell slides and
183 determined taxonomically. For the rest of the 63-150 µm samples, foraminifera were counted
184 and determined directly under the stereomicroscope. Similarly to the >150 µm fraction, samples
185 (63-150 µm) were splitted with a dry Otto microsplitter until obtaining at least 250-300
186 specimens in the final split. The benthic foraminiferal accumulation rate (ind.cm⁻².ka⁻¹)
187 (BFAR), used as paleo-productivity proxy (Herguera and Berger, 1991; Herguera, 1992;
188 Gooday, 2003; Jorissen *et al.*, 2007), was calculated for both the >150 µm and >63 µm (63-150
189 + >150 µm) fractions as: number of individuals per gram of dry sediment × linear sedimentation
190 rate (cm.ka⁻¹) × Dry Bulk Density (g.cm⁻³) (Herguera and Berger, 1991). The Dry Bulk Density
191 (DBD) was calculated following the relation: $DBD = 2.65 \times (1.024 - D_{wet}) / (1.024 - 2.65)$, where
192 2.65 g.cm⁻³ is the grain density and 1.024 g.cm⁻³ is the interstitial water density (Auffret *et al.*,
193 2002). Wet bulk densities (D_{wet}) were derived from gamma-ray attenuation density
194 measurements obtained from a 'Geotek Multi Sensor Core Logger' (MSCL).

195 The relative abundances of benthic species (% of the total foraminiferal abundances) were
196 calculated for the >150 µm fraction for the 56 samples and for the >63 µm fraction (63-150 µm
197 + >150 µm) for the selected 16 samples. The error bars of the relative abundances were
198 computed with the binomial standard error $\sqrt{(p(1-p))/n}$ (Buzas, 1990; Fatela and Taborda,
199 2002), where p is the species proportion estimate (number of counted individuals for a given
200 species/n). The diversity of the 56 samples (>150 µm) was calculated with the Shannon index

201 (entropy, H; Hayek and Buzas, 1997) using the PAST software (PAleontological STatistics;
202 Version 2.14; Hammer *et al.*, 2001). Error bars representing 95 % confidence interval were
203 computed with a bootstrap procedure. In this study, we discuss mainly the most dominant
204 species with relative abundance >10 % showing the highest variability. All species with relative
205 abundance between 5 and 10 % in at least one sample are presented in supplementary material
206 S2, and their ecological interpretations summarized in Table 2. The complete raw data set is
207 available as supplementary material S3 and in SEANOE data repository
208 (<https://doi.org/10.17882/88029>). Scanning Electron Microscope (SEM) photographs were
209 obtained at LPG (Angers University, France) using a Tabletop Microscope Hitachi
210 TM4000Plus.

211 For the counts of the planktonic taxon *N. pachyderma*, the >150 μm fraction were used and the
212 relative abundances were determined using a minimum of 300 planktonic foraminiferal tests
213 from single sample splits. Counting was performed at University of Bordeaux (France).

214

215 **4. Results**

216 Average BFAR values from the >150 μm fraction are $\sim 12 \cdot 10^3 \text{ ind.cm}^{-2} \cdot \text{ka}^{-1}$ and from the
217 >63 μm are $\sim 7.5 \cdot 10^6 \text{ ind.cm}^{-2} \cdot \text{ka}^{-1}$ (Fig. 3a). The values from the >150 μm fraction are minimal
218 during the three HSs ($\sim 1 \cdot 10^3 \text{ ind.cm}^{-2} \cdot \text{ka}^{-1}$) and are more important during the interstadial
219 periods ($\sim 30 \cdot 10^3 \text{ ind.cm}^{-2} \cdot \text{ka}^{-1}$).

220 From ~ 32 to 14 ka cal BP, the Shannon (H) index (Fig. 3b) shows an overall increase of
221 diversity, with values ranging from ~ 2 to 3.2.

222 The eight most dominant species (>10 %) showing the highest variability are illustrated in
223 Plate 1 and their relative abundances are presented in Figure 3 (c-j). *Elphidium* spp.,
224 *Cassidulina crassa* and *Cibicides lobatulus* are dominant along the record and account together
225 for 12.7 to 74.3 % of the total fauna. In this study, *Elphidium* spp. includes mainly *E. excavatum*
226 (i.e. *E. excavatum* f. *clavatum*) with pyritized shells (Plate 2a) and other species of the genus
227 *Elphidium* (e.g. *E. gerthi*, *E. macellum*). *Elphidium* spp. show maximum values (>30 %)
228 between 30.7 and 28.9 ka cal BP (i.e. HS3) and minimum values (<10 %) between 17.5 and
229 16.5 ka cal BP (i.e. Early HS1; Fig. 3c). Before HS2, *C. crassa* accounts in average for about
230 ~ 21 % of the total fauna (Fig. 3d). The highest values are recorded during HS2, with maximum
231 percentages (40 %) just before HE2 followed by a sharp decrease. After HS2, the relative
232 density of this species remains stable around ~ 8 %. *Cibicides lobatulus* exhibits a different

233 pattern in comparison with the previously mentioned species. Generally, this species is present
234 with lower proportions during HS periods (around 5-10 %), except at 24.2 ka cal BP (during
235 HE2) and 17.2 ka cal BP (during HS1). Between HS3 and HS2 (ca. 29-26 ka cal BP) and during
236 the LGM (ca. 23-18 ka cal BP), *C. lobatulus* accounts for ~22 % of the total fauna (Fig. 3e).
237 *Trifarina angulosa* shows the same trend as *C. lobatulus* (Fig. 3f) but with overall lower
238 proportions (maximum values around 10 %). The remaining dominant species (>10 %) present
239 a discontinuous evolution. *Cassidulina carinata*, *Bolivina* spp. and *Globobulimina* spp. exhibit
240 high relative abundances (up to 42 %, 24 % and 18 % respectively), with high variability,
241 during early HS1 (Figs. 3g, 3h & 3i). Before HS1, *Globobulimina* species are almost absent
242 except in samples from HS3 and HS2 (average of ~5 % and 7.5 %, respectively). *Cibicidoides*
243 *pachyderma* is also present mainly during the three HSs reaching 12.5 % at 29.3 ka cal BP (i.e.
244 during HS3), 20 % at 25.3 ka cal BP (i.e. during HS2) and varying around 10 % at ~HS1
245 (Fig. 3j). Here, *C. pachyderma* encompasses several morphotypes spanning from *C.*
246 *pachyderma* sensu stricto (pronounced carina) to *Cibicidoides kullenbergi* sensu stricto (less
247 pronounced carina) (Plate 2b). The presence of several intermediate morphotypes hampered the
248 taxonomical differentiation between *C. pachyderma* and *C. kullenbergi*, and as such were
249 lumped together as *C. pachyderma*.

250 The evolution through time of the minor species (i.e. present only few times with percentages
251 >5 %) is represented in supplementary material S2. *Gavelinopsis praegeri* and *Planorbulina*
252 *mediterraneensis* mainly appear just after 24.2 ka cal BP, between HE2 and the end of HS2.
253 *Chilostomella oolina*, *Pullenia quinqueloba*, *Textularia sagittula* occur just one time with
254 relative densities >5 % at 16.8 ka cal BP, 16.5 ka cal BP, 17.2 ka cal BP respectively while
255 *Hoeglundina elegans* occurs only at 14 ka cal BP. *Nonionella turgida* become dominant only
256 after HE1 (~6 %).

257 In the small fraction (63-150 μm), the identified species were similar to the ones found in the
258 larger size fraction (>150 μm). When considering the small and large fractions together
259 (>63 μm), six major species >5 % are present: *Elphidium* spp., *C. crassa*, *C. lobatulus*, *C.*
260 *carinata*, *Bolivina* spp. and *T. angulosa*. These species, also identified as major species when
261 considering only the >150 μm size fraction, exhibit approximately similar trends (black dashed
262 line; Fig. 3 c-h). Only *C. crassa* presents much higher proportions in the >63 μm fraction with
263 abundances ranging from 15 to 60 % of the total fauna.

264

265 **5. Discussion**

266 **5.1. Regional inter-comparison of benthic foraminiferal faunas**

267 Most of the dominant foraminiferal taxa in core BOBGEO-CS05 (e.g. *C. pachyderma*,
268 *C. carinata*, *C. crassa*, *Bolivina* spp., *Globobulimina* spp.) inhabit the modern upper slope
269 environments of the BoB (e.g. Murray, 1970; Fontanier *et al.*, 2006; Mojtahid *et al.*, 2010;
270 Duros *et al.*, 2011, 2012; Dorst and Schönfeld, 2013), and/or are found in the regional benthic
271 fossil (i.e. last glacial) records of intermediate waters depths (Fig. 1c; Mojtahid *et al.*, 2017;
272 Pascual *et al.*, 2020). However, some discrepancies are observed and detailed hereafter:

273

274 **5.1.1. High-energy indicator species**

275 *Cibicides lobatulus* (also known as *Lobatula lobatula*) is highly dominant in our record
276 (~4-30 %). This species is also present, but with overall lower percentages (~10 %), at site
277 MD99-2328, north of our study site (Fig. 1), that covers the time interval from 23 to
278 16 ka cal BP (Mojtahid *et al.*, 2017) (Fig. 3). However, this epibenthic species is absent today
279 from the BoB modern foraminiferal communities at ~1000 m depth (e.g. Fontanier *et al.*, 2002;
280 Fontanier *et al.*, 2006; Mojtahid *et al.*, 2010; Duros *et al.*, 2011, 2012). This discrepancy can be
281 explained by different environmental conditions (e.g. food source, hydrodynamics) during the
282 last glacial period allowing their settlement at intermediate water depths in the area. Indeed, *C.*
283 *lobatulus* is a suspension-feeder that inhabits moderate-to-strong hydrodynamic environments
284 of the modern northeast Atlantic. These include shelf environments (e.g. Basque shelf; Pascual
285 *et al.*, 2008) and upper slope settings swept by strong bottom currents and characterized by
286 coarse substrate and/or cold-water coral mounds and reefs trapping abundant food particles (e.g.
287 Gulf of Cadiz, Porcupine and Rockall Banks; Schönfeld, 1997, 2002a, 2002b; Margreth *et al.*,
288 2009; Spezzaferri *et al.*, 2015). As such, the high presence of *C. lobatulus* in the BOBGEO-
289 CS05 glacial record might indicate stronger currents than today. The depicted link between *C.*
290 *lobatulus* and strong energy environments is further supported in our record by its co-variation
291 with: i) the abundance of *Trifarina angulosa* ($r^2 = 0.78$) (Figs. 3e & 3f) which is commonly
292 associated with shelf-edge to upper-slope areas swept by vigorous bottom currents (e.g.
293 southwest Norway, Rockall Trough; Mackensen *et al.*, 1985; Austin and Evans, 2000; Gooday
294 and Hughes, 2002), and ii) the “sortable silt” mean size \overline{SS} (i.e. the mean grain size of the
295 carbonate-free terrigenous silt fraction) at BOBGEO-CS05 (Fig. 4f; Toucanne *et al.*, 2021) that
296 provides a direct constraint on the rate of past bottom flows (McCave *et al.*, 1995). As such,
297 our biotic data independently support the presence of strong bottom currents on the upper slope

298 of the BoB, and by extent the presence of the GEBC along the French Atlantic margin
299 (Toucanne *et al.*, 2021). Based on the above, we summed the percentages of *C. lobatulus* and
300 *T. angulosa* to constitute the group of high-energy indicator species. The latter will be used to
301 examine the hydrodynamics variability in the study area throughout the ca. 32-14 ka cal BP
302 interval, and more specifically during the HSs (cf. section 5.2).

303

304 **5.1.2. Glacier-proximal species**

305 The high dominance (up to ~40 % in the late MIS 3 and ~20 % thereafter) of elphidiids
306 in core BOBGEO-CS05 is peculiar as this group is presently found in coastal, shelf and
307 estuarine environments of the northeast Atlantic (e.g. Pujos, 1976; Murray, 2014; Mojtahid *et*
308 *al.*, 2016). In the modern benthic foraminiferal assemblage of the upper Whittard region
309 (northern BoB, ~1000 m depth; Duros *et al.*, 2012), *Elphidium* spp. are found only in the dead
310 faunas, and as such, were considered as transported from shallower settings. Mojtahid *et al.*
311 (2017) report high abundances of *Elphidium* spp. in core MD99-2328 especially during the late
312 HS1 (16.7-16 ka cal BP; up to ~70 %) and hypothesized their transport to these intermediate
313 depths by the EIS icebergs and/or shelf ice. This would be also a possibility for BOBGEO-
314 CS05 since *Elphidium* shells show pyritization marks (Plate 2a) that may indicate a potential
315 reworking and transport. However, it is interesting to note that modern elphidiids may extend
316 their habitats to deeper settings (several hundred meters) in cold, arctic environments, usually
317 in connection with freshwater river outflow (e.g. Bergsten, 1994; Polyak *et al.*, 2002).
318 Therefore, another explanation for the high abundance of elphidiids in the glacial BOBGEO-
319 CS05 record could simply be an adaptation to cold glacial conditions and meltwater inputs in
320 the BoB. This is supported by the presence of *E. excavatum* f. *clavatum*, the dominant elphidiids
321 species in our assemblages (~75 %), frequently found today in glacier-proximal environments
322 (e.g. Jennings *et al.*, 2004; Murray, 2006; Darling *et al.*, 2016; Fossile *et al.*, 2020). The modern
323 conditions in the polar regions where this species lives today are close to the conditions
324 prevailing during the last glacial period in our study area since the EIS invaded the western
325 European shelf (cf. ice-sheet and polar fronts limits in Fig. 1) and the Channel River channeled
326 huge amounts of meltwaters to the northern BoB.

327 *Cassidulina crassa* occurs concomitantly to *E. excavatum* f. *clavatum* in our record (r^2
328 = 0.85). Similarly to *Elphidium* spp., modern upper slope foraminiferal studies from the BoB
329 reported that *C. crassa* is either only encountered in the dead faunas or very rarely present in
330 the living faunas (e.g. Fontanier *et al.*, 2002, 2006; Mojtahid *et al.*, 2010; Duros *et al.*, 2012).

331 It is therefore probable that this species has been transported to the study site, although *C. crassa*
332 tests are rather intact (Plate 1) compared to *E. excavatum* f. *clavatum* (Plate 2a). It must be noted
333 that the morphospecies identified here as *C. crassa* (d'Orbigny, 1839) has a variant that is very
334 close morphologically and was described first as *Cassidulina crassa* var. *reniforme* Nørvang,
335 1945, and later elevated to the species rank as *C. reniforme*. *Cassidulina reniforme*
336 morphospecies is mainly reported from arctic regions as typical of near-glacier environments
337 (Hansen and Knudsen, 1995; Korsun *et al.*, 1995; Murray, 2006). Thus, it is highly possible
338 that *C. crassa* from BOBGEO-CS05 is actually the same morphospecies than the one reported
339 from arctic regions. We therefore assume that the *C. crassa* - *E. excavatum* f. *clavatum*
340 association in our record is coherent with near-glacier environments. This is further
341 corroborated by the absence of these species in the upper slope glacial record PP10-12 from the
342 southeast BoB (Pascual *et al.*, 2020), far from both the ice sheet extent limit and the Channel
343 River mouth. Based on the above, we summed the percentages of *E. excavatum* f. *clavatum* and
344 *C. crassa* to constitute the group of glacier-proximal indicator species. The latter will be used
345 to examine the EIS dynamics (cf. section 5.2).

346

347 **5.1.3. Holocene indicator species**

348 One of the most striking features of our benthic foraminiferal record is the absence of
349 uvigerinids (e.g. *U. peregrina*, *U. mediterranea*), whereas they dominate the modern benthic
350 foraminiferal assemblages of the BoB between ~500 and 2000 m water depth (e.g., Schönfeld,
351 2006; Barras *et al.*, 2010; Mojtahid *et al.*, 2010; Duros *et al.*, 2011, 2012). This absence is also
352 the case in the glacial part of the MD99-2328 record (Mojtahid *et al.*, 2017). We assume
353 therefore that uvigerinids might not be tolerant to the glacial-related conditions on the BoB
354 seafloor (Mojtahid *et al.*, 2013; Pascual *et al.*, 2020; Rodriguez-Lazaro *et al.*, 2017). Schönfeld
355 and Altenbach (2005) hypothesized a widespread change from glacial to modern surface
356 productivity configuration (e.g. nature of primary producers, seasonality in phytoplankton
357 blooms) that may have triggered the Holocene settlement of *U. peregrina* in the northeast
358 Atlantic. It is also interesting to note that *U. peregrina* and *U. mediterranea* are very abundant
359 in bathyal depths (~200-1500 m) of the Mediterranean and the BoB bathed by the MOW (e.g.
360 De Rijk *et al.*, 2000; Schmiedl *et al.*, 2000; Fontanier *et al.*, 2003). The possible link between
361 water masses and specific fauna has been progressively abandoned in favor of organic matter
362 and oxygen as major controlling environmental parameters (Jorissen *et al.*, 2007). Yet, the
363 settlement of uvigerinids in the BoB in the end of deglaciation - early Holocene (Garcia *et al.*,

364 2013; Mojtahid *et al.*, 2013; Pascual *et al.*, 2020) seems to coincide with the significant increase
365 in the influx of the MOW into the North Atlantic and along the European margin (Rogerson *et*
366 *al.*, 2012; Lebreiro *et al.*, 2018). This is coherent with what Mojtahid *et al.* (2017) observed in
367 core MD99-2328 where they record the appearance of uvigerinids (although with low
368 abundances) only in the Holocene portion of the record.

369

370 In summary, we have shown that the upper slope benthic foraminifera assemblage found at site
371 BOBGEO-CS05 reflect the complex, highly dynamic and variable environmental conditions in
372 the northern BoB during the last glacial period, including high bottom water currents, glacier-
373 proximal settings, and southern retreat of the MOW. Since benthic foraminifera respond greatly
374 to these various environmental parameters, they present a great potential to better constrain
375 glacial intermediate bottom water characteristics during HSs.

376

377 ***5.2. Environmental particularities of Heinrich Stadials depicted by benthic*** 378 ***foraminifera***

379 **5.2.1. What do the last three Heinrich Stadials have in common in the Bay of** 380 **Biscay?**

381 In general, HS3 (~31-29 ka cal BP), HS2 (~26-23 ka cal BP) and HS1 (~18-
382 15.5 ka cal BP) in core BOBGEO-CS05 are characterized by a systematic drop in BFAR values
383 (Fig. 3a). This may indicate unfavorable conditions (e.g. low quality/quantity of the organic
384 matter, low oxygenation) for the growth and reproduction of foraminifera. In the same intervals,
385 we record the highest occurrence of *Cibicidoides pachyderma* and *Globobulimina* spp. (Figs. 3j
386 & 3i). *Cibicidoides pachyderma* is usually found in meso-oligotrophic open-slope
387 environments, as in the modern BoB (Schmiedl *et al.*, 2000; Mojtahid *et al.*, 2010; Duros *et al.*,
388 2012). *Globobulimina* spp., on the other hand, are deep infaunal species that tolerate hypoxia
389 and anoxia (Risgaard-Petersen *et al.*, 2006; Pina-Ochoa *et al.*, 2010; Koho *et al.*, 2011). Hence,
390 we interpret the *C. pachyderma* - *Globobulimina* spp. association (i.e. meso-oligotrophic
391 species; see Fig. 4h) during HSs, together with the low BFAR, as indicating meso-oligotrophic
392 conditions, with moderate to low export of organic matter to the seafloor, and reduced bottom-
393 water ventilation. The latter is supported by the concomitant decrease in the proportions of
394 high-energy indicator species *T. angulosa* and *C. lobatulus* during each of the HSs (Fig. 4g).
395 The weak hydrodynamics during the HSs is independently supported by the low \overline{SS} values at
396 BOBGEO-CS05 and at many sites along the French Atlantic margin (Toucanne *et al.*, 2021).

397 As such, biotic and sedimentological data indicate reduced near-bottom flow speed (i.e.
398 weakened GEBC) and, by extension, a sluggish AMOC during the three HSs.
399 The glacier-proximal species (*E. excavatum* f. *clavatum*. and *C. crassa*), although present all
400 along the BOBGEO-CS05 record, display the highest percentages during the HSs, especially
401 during HS3 and HS2 (Fig. 4b). In their modern habitats in the Arctic fjords, these species are
402 impacted by seasonal melting of marine-terminating glaciers (Schroder-Adams *et al.*, 1990;
403 Wollenburg and Mackensen, 1998; Wollenburg and Kuhnt, 2000; Wollenburg *et al.*, 2004).
404 Since enhanced EIS meltwaters influx to the BoB are described during HSs (Toucanne *et al.*,
405 2015), increased densities of these species might be indicative of such meltwater inputs. The
406 concomitant presence of meso-oligotrophic species (e.g. *C. pachyderma*) indicates a low to
407 moderate export of organic matter to the seafloor, especially during HS2 and HS3. This will be
408 further discussed when addressing the specificities of each HS (cf. sections 5.2.2. and 5.3)

409

410 **5.2.2. The difference between the early HS1 and the other HSs**

411 In core BOBGEO-CS05, HS1 is very distinct from HS2 and HS3 by displaying a high presence
412 (~60 %) of opportunistic and high-organic flux indicator species (*C. carinata* and *Bolivina* spp.;
413 Schmiedl *et al.*, 1997; Fontanier *et al.*, 2003; Duros *et al.*, 2011) during its early phase ca. ~18-
414 16.7 ka cal BP (Fig. 4d). This is coherent with the findings of Mojtahid *et al.* (2017) at the same
415 time period at site MD99-2328. Conversely, during HS2 and HS3, these species were present
416 with much lower abundances (< 10 %; Fig. 4d). Thus, we assume that limited organic material
417 inputs reached the BOBGEO-CS05 site during HS3 and HS2, then substantially increased
418 during the early HS1. This difference is further corroborated by the positive correlation between
419 the abundance of the high-organic flux indicator species during early HS1 at our site and both
420 the BIT index at site MD95-2002 (Fig. 4c; Ménot *et al.*, 2006) and the turbidite (i.e. flood-
421 related deposits) flux in the deep BoB (Zaragosi *et al.*, 2006; Toucanne *et al.*, 2008, 2012). It
422 has been suggested that these differences in organic material inputs through time could result
423 from complex interactions between climate conditions, and ice and vegetation cover (Ménot *et al.*,
424 2006). Our data cannot resolve this issue, but it certainly highlights the paroxysmal phase
425 of EIS melting in response to increasing boreal insolation during HS1, and the concomitant
426 rapid progradation of a large outer-shelf delta that ultimately improved the connection between
427 the BOBGEO-CS05 site and the Channel River system (Toucanne *et al.*, 2012). That said,
428 because *C. carinata* and *Bolivina* spp. are very abundant in shallower settings in the BoB (140-
429 550 m depth; Duros *et al.*, 2011 ; Fontanier *et al.*, 2003), we cannot discard that their presence

430 in our record is a result of downslope transport. Even so, the abundance of these species still
431 indicates increased organic fluxes in their source habitats.
432 Interestingly, in the upper slope BOBGEO-CS05 and MD99-2328 cores, the dominance of the
433 anoxia indicator species (representing the sum of *Globobulimina* spp. and *Chilostomella*
434 *oolina*) at HS1 occurs early within this interval, before HE1 event *sensu stricto* (Fig. 4i).
435 According to Mojtahid *et al.* (2017), the presence of these indicator species during early HS1
436 is indicative of organically-enriched and/or oxygen-depleted benthic environments, and their
437 absence during HE1 event, together with high \overline{SS} (Fig. 4i & 4f) indicate well-ventilated
438 intermediate waters. In deeper sediment cores from the BoB (>2000 m depth), the HE1 event
439 is characterized by the presence of authigenic carbonates indicating anoxic bottom waters (e.g.
440 Auffret *et al.*, 1996; Toucanne *et al.*, 2015). Because these anoxia markers are not observed in
441 the shallower cores BOBGEO-CS05 and MD99-2328 and because all proxies (\overline{SS} and
442 foraminifera; Fig. 4) indicate well-ventilated bottom waters, we can hypothesize a decoupling
443 between a vigorous intermediate water depth circulation during HE1 and a still sluggish
444 circulation at >2000 m in the northeast Atlantic, as reported by the Bermuda rise $^{231}\text{Pa}/^{230}\text{Th}$
445 data from the deep northwest Atlantic (Fig. 4e). A similar pattern is found in the equatorial
446 Atlantic where a better ventilation of mid-depth waters in late HS1 is recorded while the deep
447 sites remained poorly ventilated (Chen *et al.*, 2015).

448

449 **5.3. Foraminiferal evidence for mid-HS2 re-ventilation event**

450 During HS2 (Fig. 5), the overall meso-oligotrophic conditions and the low bottom-water
451 ventilation depicted by both the low BFAR and the *C. pachyderma* - *Globobulimina* spp.
452 association (i.e. meso-oligotrophic species) were interrupted around 24.3 ka cal BP (Fig. 5d
453 & 5e). At the same time, low percentages of the polar planktonic species *N. pachyderma*
454 (Fig. 5a) indicate a a warming of the sea-surface conditions and therefore a cessation of
455 meltwater input in the northern BoB. This surface water warming is recorded in several
456 sedimentary records along the European margin (e.g. Scourse *et al.*, 2009; Austin *et al.*, 2012;
457 Waelbroeck *et al.*, 2019). This warm event interrupting HS2 seems to be coeval with a well-
458 known atmospheric decrease in dust flux at high latitudes (Rasmussen *et al.*, 2008; Austin *et*
459 *al.*, 2012). During this sea-surface warming event, the re-appearance of the high-energy
460 indicator species (Fig. 5c) and the drop in the anoxia indicator species (Fig. 5f) strongly
461 suggests a reactivation of bottom water currents at site BOBGEO-CS05. This is supported by
462 the increase in the \overline{SS} values at our site and, more generally, in the northern part of the French

463 Atlantic margin (Fig. 5b;). Our biotic data, although covering this millennial-scale event at low
464 sampling resolution, thus indicate, together with the \overline{SS} proxy, enhanced vigor of the GEBC
465 and, by extension, of the AMOC during the mid-HS2. This re-acceleration of the GEBC
466 continues to about 100 yrs before the iceberg debacle of the LIS (i.e. HE2 *sensu stricto* at
467 24.2 ka cal BP), when our biotic and sedimentological proxies show a rapid return to meso-
468 oligotrophic conditions at the sea-floor and weak bottom currents.

469

470 **6. Conclusions**

471 Benthic foraminiferal assemblage data allowed us to reconstruct the paleoenvironmental
472 evolution of the upper slope of the BoB (site BOBGEO-CS05) over the ca. 32-14 ka cal BP
473 period. In general, species-specific responses reflect the complex, highly dynamic and variable
474 environmental conditions in the northern BoB during the last glacial period, including
475 fluctuations in the bottom water current and the GEBC, changes in organic matter fluxes and
476 Channel River discharges, and latitudinal changes of the MOW.

477 The three HSs (HS3, HS2 and HS1) present some common features. They are all
478 characterized by an overall low proportion of high-energy indicator species (i.e. *Cibicides*
479 *lobatulus* and *Trifarina angulosa*), and a significant presence of meso-oligotrophic indicator
480 species (*Cibicidoides pachyderma*), anoxia indicator species (*Globobulimina* spp. and *C.*
481 *oolina*), and glacier-proximal species (*E. excavatum* f. *clavatum* and *Cassidulina crassa*). In
482 agreement with previously published sedimentological and geochemical proxies, this reflects
483 overall low organic matter fluxes to the seafloor and a low bottom water ventilation during the
484 HSs.

485 Detailed investigation of the benthic foraminifera reveals some specificities of the HSs
486 in the northeast Atlantic. First, the high abundance of high-organic flux indicator species
487 (*Cassidulina carinata* and *Bolivina* spp.) during early HS1, compared to their near absence
488 during HS2 and HS3, reveals a millennial-scale peak in terrestrial organic material in the BoB
489 resulting from the significant EIS melting and Channel River meltwater floods. Second, benthic
490 foraminiferal species depict a short-term mid-depth re-ventilation event during HS2, indicated
491 by a decrease in the proportions of anoxia indicator species and an increase in the abundance
492 of high-energy indicator species. This short-term reactivation of the GEBC along the French
493 Atlantic margin, and of the AMOC, is coherent with the cessation of the EIS meltwater input
494 in the northern BoB, and more generally, with a warming of the sea-surface conditions in the
495 northeast Atlantic. This result strongly emphasizes the connection between the intermediate

496 ocean circulation and the cryosphere dynamics in the northeast Atlantic during the Heinrich
497 Stadials.

498

499 **7. Acknowledgments**

500 This study was funded by the CNRS-INSU-LEFE-IMAGO program (STING project), the
501 ARTEMIS ¹⁴C AMS French INSU project, and the Region Pays de Loire programs (New
502 Research Group initiative and Rising Star project TANDEM). S.T. was funded by French
503 National Research Agency (ANR) via the LabexMER program (ANR-10-LABX-19-01) and
504 the PIA TANDEM project (ANR-11-RSNR-00023-01). Salary and research support for the
505 PhD student (First author) were provided by the French Ministry of Higher Education and
506 Research. We thank S. Le Houedec for core sampling, and L. Rossignol and S. Zaragosi
507 (University of Bordeaux) for planktonic foraminifera counting, respectively. Finally, the
508 authors warmly acknowledge J.-F. Bourillet (Ifremer), P.I. of the BOBGEO cruise
509 (doi.org/10.17600/9030060), for his strong support on this research project

510

511 **8. References**

- 512 Allen, K.A., Hönisch, B., Eggins, S.M., Haynes, L.L., Rosenthal, Y., Yu, J., 2016. Trace element proxies for
513 surface ocean conditions: A synthesis of culture calibrations with planktic foraminifera. *Geochimica et*
514 *Cosmochimica Acta* 193, 197–221. <https://doi.org/10.1016/j.gca.2016.08.015>
- 515 Altenbach, A.V., Pflaumann, U., Schiebel, R., Thies, A., Timm, S., Trauth, M., 1999. Scaling percentages and
516 distributional patterns of benthic Foraminifera with flux rates of organic carbon. *Journal of Foraminiferal*
517 *Research* 29, 173–185.
- 518 Alvarez-Solas, J., Robinson, A., Montoya, M., Ritz, C., 2013. Iceberg discharges of the last glacial period driven
519 by oceanic circulation changes. *PNAS* 110, 16350–16354. <https://doi.org/10.1073/pnas.1306622110>
- 520 Auffret, G., Zaragosi, S., Dennielou, B., Cortijo, E., Van Rooij, D., Grousset, F., Pujol, C., Eynaud, F., Siebert,
521 M., 2002. Terrigenous fluxes at the Celtic margin during the last glacial cycle. *Marine Geology* 188, 79–108.
522 [https://doi.org/10.1016/S0025-3227\(02\)00276-1](https://doi.org/10.1016/S0025-3227(02)00276-1)
- 523 Auffret, G.A., Boelaert, A., Vergnaud-Grazzini, C., Müller, C., Kerbrat, R., 1996. Identification of Heinrich
524 Layers in core KS 01 North-Eastern Atlantic (46 °N, 17 °W), implications for their origin. *Marine Geology, Ice*
525 *Rafting and Paleoenvironment of the Northeast Atlantic Ocean Selected papers presented at the 7th European*
526 *Union of Geosciences* 131, 5–20. [https://doi.org/10.1016/0025-3227\(95\)00141-7](https://doi.org/10.1016/0025-3227(95)00141-7)
- 527 Austin, W.E.N., Evans, J.R., 2000. NE Atlantic benthic foraminifera: modern distribution patterns and
528 palaeoecological significance. *Journal of the Geological Society* 157, 679–691.
529 <https://doi.org/10.1144/jgs.157.3.679>
- 530 Austin, W.E.N., Hibbert, F.D., Rasmussen, S.O., Peters, C., Abbott, P.M., Bryant, C.L., 2012. The
531 synchronization of palaeoclimatic events in the North Atlantic region during Greenland Stadial 3 (ca 27.5 to 23.3
532 kyr b2k). *Quat. Sci. Rev.* 36, 154–163. <https://doi.org/10.1016/j.quascirev.2010.12.014>

- 533 Bard, E., Rostek, F., Turon, J.-L., Gendreau, S., 2000. Hydrological Impact of Heinrich Events in the Subtropical
534 Northeast Atlantic. *Science* 289, 1321–1324. <https://doi.org/10.1126/science.289.5483.1321>
- 535 Barras, C., Fontanier, C., Jorissen, F., Hohenegger, J., 2010. A comparison of spatial and temporal variability of
536 living benthic foraminiferal faunas at 550m depth in the Bay of Biscay. *Micropaleontology* 56, 275–295.
- 537 Bergsten, H., 1994. Recent benthic foraminifera of a transect from the North Pole to the Yermak Plateau, eastern
538 central Arctic Ocean. *Marine Geology*, 4th International Conference on Paleoceanography (ICP IV) 119, 251–
539 267. [https://doi.org/10.1016/0025-3227\(94\)90184-8](https://doi.org/10.1016/0025-3227(94)90184-8)
- 540 Bernhard, J.M., 1992. Benthic foraminiferal distribution and biomass related to pore-water oxygen content:
541 central California continental slope and rise. *Deep Sea Research Part A. Oceanographic Research Papers* 39,
542 585–605. [https://doi.org/10.1016/0198-0149\(92\)90090-G](https://doi.org/10.1016/0198-0149(92)90090-G)
- 543 Bernhard, J.M., Sen Gupta, Barun K., 2003. Foraminifera of oxygen-depleted environments, in: Sen Gupta,
544 Barun K. (Ed.), *Modern Foraminifera*. Springer Netherlands, Dordrecht, pp. 201–216. [https://doi.org/10.1007/0-](https://doi.org/10.1007/0-306-48104-9_12)
545 [306-48104-9_12](https://doi.org/10.1007/0-306-48104-9_12)
- 546 Berx, B., Hansen, B., Østerhus, S., Larsen, K.M., Sherwin, T., Jochumsen, K., 2013. Combining in situ
547 measurements and altimetry to estimate volume, heat and salt transport variability through the Faroe–Shetland
548 Channel. *Ocean Science* 9, 639–654. <https://doi.org/10.5194/os-9-639-2013>
- 549 Böhm, E., Lippold, J., Gutjahr, M., Frank, M., Blaser, P., Antz, B., Fohlmeister, J., Frank, N., Andersen, M.B.,
550 Deininger, M., 2015. Strong and deep Atlantic meridional overturning circulation during the last glacial cycle.
551 *Nature* 517, 73–76. <https://doi.org/10.1038/nature14059>
- 552 Bond, G., Broecker, W., Johnsen, S., McManus, J., Labeyrie, L., Jouzel, J., Bonani, G., 1993. Correlations
553 between climate records from North Atlantic sediments and Greenland ice. *Nature* 365, 143–147.
554 <https://doi.org/10.1038/365143a0>
- 555 Boswell, S.M., Toucanne, S., Pitel-Roudaut, M., Creyts, T.T., Eynaud, F., Bayon, G., 2019. Enhanced surface
556 melting of the Fennoscandian Ice Sheet during periods of North Atlantic cooling. *Geology* 47, 664–668.
557 <https://doi.org/10.1130/G46370.1>
- 558 Bourillet, J.-F., 2009. BOBGEO cruise, Pourquoi pas ? R/V. <https://doi.org/10.17600/9030060>
- 559 Bourillet, J.-F., Lericolais, G., 2003. Morphology and Seismic Stratigraphy of the Manche Paleoriver System,
560 Western Approaches, in: Mienert, J., Weaver, P. (Eds.), *European Margin Sediment Dynamics: Side-Scan Sonar*
561 *and Seismic Images*. Springer, Berlin, Heidelberg, pp. 229–232. https://doi.org/10.1007/978-3-642-55846-7_37
- 562 Brady, E.C., Otto-Bliesner, B.L., 2011. The role of meltwater-induced subsurface ocean warming in regulating
563 the Atlantic meridional overturning in glacial climate simulations. *Clim Dyn* 37, 1517–1532.
564 <https://doi.org/10.1007/s00382-010-0925-9>
- 565 Broecker, W.S., Denton, G.H., 1990. The role of ocean-atmosphere reorganizations in glacial cycles. *Quaternary*
566 *Science Reviews* 9, 305–341. [https://doi.org/10.1016/0277-3791\(90\)90026-7](https://doi.org/10.1016/0277-3791(90)90026-7)
- 567 Buckley, M.W., Marshall, J., 2016. Observations, inferences, and mechanisms of the Atlantic Meridional
568 Overturning Circulation: A review. *Reviews of Geophysics* 54, 5–63. <https://doi.org/10.1002/2015RG000493>
- 569 Buzas, M.A., 1990. Another look at confidence limits for species proportions. *Journal of Paleontology* 64, 842–
570 843. <https://doi.org/10.1017/S002233600001903X>
- 571 Chen, T., Robinson, L.F., Burke, A., Southon, J., Spooner, P., Morris, P.J., Ng, H.C., 2015. Synchronous
572 centennial abrupt events in the ocean and atmosphere during the last deglaciation. *Science*.
573 <https://doi.org/10.1126/science.aac6159>
- 574 Clark, C.D., Hughes, A.L.C., Greenwood, S.L., Jordan, C., Sejrup, H.P., 2012. Pattern and timing of retreat of
575 the last British-Irish Ice Sheet. *Quaternary Science Reviews, Quaternary Glaciation History of Northern Europe*
576 44, 112–146. <https://doi.org/10.1016/j.quascirev.2010.07.019>

- 577 Clark, M., Marsh, R., Harle, J., 2021. Weakening and warming of the European Slope Current since the late
578 1990s attributed to basin-scale density changes (preprint). Shelf-sea depth/Data Assimilation/Shelf
579 Seas/Transports/cycling (nutrients, C, O, etc.)/Ocean-shelf interactions. <https://doi.org/10.5194/os-2021-60>
- 580 Corliss, B.H., 1991. Morphology and microhabitat preferences of benthic foraminifera from the northwest
581 Atlantic Ocean. *Marine Micropaleontology* 17, 195–236. [https://doi.org/10.1016/0377-8398\(91\)90014-W](https://doi.org/10.1016/0377-8398(91)90014-W)
- 582 Corliss, B.H., Emerson, S., 1990. Distribution of rose bengal stained deep-sea benthic foraminifera from the
583 Nova Scotian continental margin and Gulf of Maine. *Deep Sea Research Part A. Oceanographic Research Papers*
584 37, 381–400. [https://doi.org/10.1016/0198-0149\(90\)90015-N](https://doi.org/10.1016/0198-0149(90)90015-N)
- 585 Crocker, A.J., Chalk, T.B., Bailey, I., Spencer, M.R., Gutjahr, M., Foster, G.L., Wilson, P.A., 2016.
586 Geochemical response of the mid-depth Northeast Atlantic Ocean to freshwater input during Heinrich events 1 to
587 4. *Quaternary Science Reviews* 151, 236–254. <https://doi.org/10.1016/j.quascirev.2016.08.035>
- 588 Darling, K.F., Schweizer, M., Knudsen, K.L., Evans, K.M., Bird, C., Roberts, A., Filipsson, H.L., Kim, J.-H.,
589 Gudmundsson, G., Wade, C.M., Sayer, M.D.J., Austin, W.E.N., 2016. The genetic diversity, phylogeography
590 and morphology of Elphidiidae (Foraminifera) in the Northeast Atlantic. *Marine Micropaleontology* 129, 1–23.
591 <https://doi.org/10.1016/j.marmicro.2016.09.001>
- 592 De Rijk, S., Jorissen, F.J., Rohling, E.J., Troelstra, S.R., 2000. Organic flux control on bathymetric zonation of
593 Mediterranean benthic foraminifera. *Marine Micropaleontology* 40, 151–166. [https://doi.org/10.1016/S0377-8398\(00\)00037-2](https://doi.org/10.1016/S0377-8398(00)00037-2)
- 595 de Stigter, H.C., 1996. Recent and fossil benthic foraminifera in the Adriatic Sea: distribution patterns in relation
596 to organic carbon flux and oxygen concentration at the seabed [WWW Document]. URL
597 <http://dspace.library.uu.nl/handle/1874/315842> (accessed 5.13.22).
- 598 de Stigter, H.C., Jorissen, F.J., van der Zwaan, G.J., 1998. Bathymetric distribution and microhabitat partitioning
599 of live (Rose Bengal stained) benthic Foraminifera along a shelf to bathyal transect in the southern Adriatic Sea.
600 *Journal of Foraminiferal Research* 28, 40–65.
- 601 Denton, G., Anderson, R., Toggweiler, J.R., Edwards, R., Schaefer, J., Putnam, A., 2010. The Last Glacial
602 Termination. *Science (New York, N.Y.)* 328, 1652–6. <https://doi.org/10.1126/science.1184119>
- 603 Denton, G.H., Putnam, A.E., Russell, J.L., Barrell, D.J.A., Schaefer, J.M., Kaplan, M.R., Strand, P.D., 2021. The
604 Zealandia Switch: Ice age climate shifts viewed from Southern Hemisphere moraines. *Quaternary Science*
605 *Reviews* 257, 106771. <https://doi.org/10.1016/j.quascirev.2020.106771>
- 606 Dickson, R.R., Brown, J., 1994. The production of North Atlantic Deep Water: Sources, rates, and pathways.
607 *Journal of Geophysical Research: Oceans* 99, 12319–12341. <https://doi.org/10.1029/94JC00530>
- 608 Dorst, S., Schönfeld, J., 2013. Diversity of benthic foraminifera on the shelf and slope of the NE Atlantic :
609 analysis of Datasets. *Journal of Foraminiferal Research* 43, 238–254. <https://doi.org/10.2113/gsjfr.43.3.238>
- 610 Dorst, S., Schönfeld, J., Walter, L., 2015. Recent benthic foraminiferal assemblages from the Celtic Sea (South
611 Western Approaches, NE Atlantic). *Paläontol Z* 89, 287–302. <https://doi.org/10.1007/s12542-014-0240-6>
- 612 Duros, P., Fontanier, C., de Stigter, H.C., Cesbron, F., Metzger, E., Jorissen, F.J., 2012. Live and dead benthic
613 foraminiferal faunas from Whittard Canyon (NE Atlantic): Focus on taphonomic processes and paleo-
614 environmental applications. *Marine Micropaleontology* 94–95, 25–44.
615 <https://doi.org/10.1016/j.marmicro.2012.05.004>
- 616 Duros, P., Fontanier, C., Metzger, E., Pusceddu, A., Cesbron, F., de Stigter, H.C., Bianchelli, S., Danovaro, R.,
617 Jorissen, F.J., 2011. Live (stained) benthic foraminifera in the Whittard Canyon, Celtic margin (NE Atlantic).
618 *Deep Sea Research Part I: Oceanographic Research Papers* 58, 128–146.
619 <https://doi.org/10.1016/j.dsr.2010.11.008>
- 620 Duros, P., Silva Jacinto, R., Dennielou, B., Schmidt, S., Martinez Lamas, R., Gautier, E., Roubi, A., Gayet, N.,
621 2017. Benthic foraminiferal response to sedimentary disturbance in the Capbreton canyon (Bay of Biscay, NE

- 622 Atlantic). *Deep Sea Research Part I: Oceanographic Research Papers* 120, 61–75.
623 <https://doi.org/10.1016/j.dsr.2016.11.012>
- 624 Eynaud, F., Malaizé, B., Zaragosi, S., Vernal, A. de, Scourse, J., Pujol, C., Cortijo, E., Grousset, F.E., Penaud,
625 A., Toucanne, S., Turon, J.-L., Auffret, G., 2012. New constraints on European glacial freshwater releases to the
626 North Atlantic Ocean. *Geophysical Research Letters* 39. <https://doi.org/10.1029/2012GL052100>
- 627 Fatela, F., Taborda, R., 2002. Confidence limits of species proportions in microfossil assemblages. *Marine*
628 *Micropaleontology* 45, 169–174. [https://doi.org/10.1016/S0377-8398\(02\)00021-X](https://doi.org/10.1016/S0377-8398(02)00021-X)
- 629 Fontanier, C., Jorissen, F., Anschutz, P., Chaillou, G., 2006. Seasonal variability of benthic foraminiferal faunas
630 at 1000 m depth in the Bay of Biscay. *Journal of Foraminiferal Research* 36, 61–76.
631 <https://doi.org/10.2113/36.1.61>
- 632 Fontanier, C., Jorissen, F.J., Chaillou, G., Anschutz, P., Grémare, A., Griveaud, C., 2005. Live foraminiferal
633 faunas from a 2800m deep lower canyon station from the Bay of Biscay: Faunal response to focusing of
634 refractory organic matter. *Deep Sea Research Part I: Oceanographic Research Papers* 52, 1189–1227.
635 <https://doi.org/10.1016/j.dsr.2005.01.006>
- 636 Fontanier, C., Jorissen, F.J., Chaillou, G., David, C., Anschutz, P., Lafon, V., 2003. Seasonal and interannual
637 variability of benthic foraminiferal faunas at 550m depth in the Bay of Biscay. *Deep Sea Research Part I:*
638 *Oceanographic Research Papers* 50, 457–494. [https://doi.org/10.1016/S0967-0637\(02\)00167-X](https://doi.org/10.1016/S0967-0637(02)00167-X)
- 639 Fontanier, C., Jorissen, F.J., Licari, L., Alexandre, A., Anschutz, P., Carbonel, P., 2002. Live benthic
640 foraminiferal faunas from the Bay of Biscay: faunal density, composition, and microhabitats. *Deep Sea Research*
641 *Part I: Oceanographic Research Papers* 49, 751–785. [https://doi.org/10.1016/S0967-0637\(01\)00078-4](https://doi.org/10.1016/S0967-0637(01)00078-4)
- 642 Fontanier, C., Jorissen, F.J., Michel, E., Cortijo, E., Vidal, L., Anschutz, P., 2008. Stable oxygen and carbon
643 isotopes of live (stained) benthic foraminifera from cap-ferret canyon (bay of biscay). *Journal of Foraminiferal*
644 *Research* 38, 39–51. <https://doi.org/10.2113/gsjfr.38.1.39>
- 645 Fossile, E., Nardelli, M.P., Jouini, A., Lansard, B., Pusceddu, A., Moccia, D., Michel, E., Péron, O., Howa, H.,
646 Mojtahid, M., 2020. Benthic foraminifera as tracers of brine production in the Storfjorden “sea ice factory.”
647 *Biogeosciences* 17, 1933–1953. <https://doi.org/10.5194/bg-17-1933-2020>
- 648 Friocourt, Y., Levier, B., Speich, S., Blanke, B., Drijfhout, S.S., 2007. A regional numerical ocean model of the
649 circulation in the Bay of Biscay. *Journal of Geophysical Research: Oceans* 112.
650 <https://doi.org/10.1029/2006JC003935>
- 651 Garcia, J., Mojtahid, M., Howa, H., Michel, E., Schiebel, R., Charbonnier, C., Anschutz, P., Jorissen, F.J., 2013.
652 Benthic and Planktic Foraminifera as Indicators of Late Glacial to Holocene Paleoclimatic Changes in a
653 Marginal Environment: An Example from the Southeastern Bay of Biscay. *Acta Protozoologica* 52.
- 654 Gooday, A.J., 2003. Benthic foraminifera (protista) as tools in deep-water palaeoceanography: Environmental
655 influences on faunal characteristics, in: *Advances in Marine Biology*. Academic Press, pp. 1–90.
656 [https://doi.org/10.1016/S0065-2881\(03\)46002-1](https://doi.org/10.1016/S0065-2881(03)46002-1)
- 657 Gooday, A.J., Hughes, J.A., 2002. Foraminifera associated with phytodetritus deposits at a bathyal site in the
658 northern Rockall Trough (NE Atlantic): seasonal contrasts and a comparison of stained and dead assemblages.
659 *Marine Micropaleontology* 46, 83–110. [https://doi.org/10.1016/S0377-8398\(02\)00050-6](https://doi.org/10.1016/S0377-8398(02)00050-6)
- 660 Grousset, F.E., Pujol, C., Labeyrie, L., Auffret, G., Boelaert, A., 2000. Were the North Atlantic Heinrich events
661 triggered by the behavior of the European ice sheets? *Geology* 28, 123–126. [https://doi.org/10.1130/0091-7613\(2000\)28<123:WTNAHE>2.0.CO;2](https://doi.org/10.1130/0091-7613(2000)28<123:WTNAHE>2.0.CO;2)
- 663 Gupta, A.K., 1999. Latest Pliocene through Holocene paleoceanography of the eastern Indian Ocean: benthic
664 foraminiferal evidence. *Marine Geology* 161, 63–73. [https://doi.org/10.1016/S0025-3227\(99\)00056-0](https://doi.org/10.1016/S0025-3227(99)00056-0)
- 665 Hammer, O., Harper, D.A.T., Ryan, P.D., 2001. PAST: Paleontological Statistics Software Package for
666 Education and Data Analysis 9.

- 667 Hansen, A., Knudsen, K.L., 1995. Recent foraminiferal distribution in Freemansundet and Early Holocene
668 stratigraphy on Edgeøya, Svalbard. *Polar Research* 14, 215–238. <https://doi.org/10.3402/polar.v14i2.6664>
- 669 Hayek, L.-A., Buzas, M., 1997. *Surveying Natural Populations: Quantitative Tools for Assessing Biodiversity*,
670 *Surveying Natural Populations*. Columbia University Press. <https://doi.org/10.7312/haye14620>
- 671 Hemming, S.R., 2004. Heinrich events: Massive late Pleistocene detritus layers of the North Atlantic and their
672 global climate imprint. *Reviews of Geophysics* 42. <https://doi.org/10.1029/2003RG000128>
- 673 Henry, L.G., McManus, J.F., Curry, W.B., Roberts, N.L., Piotrowski, A.M., Keigwin, L.D., 2016. North Atlantic
674 ocean circulation and abrupt climate change during the last glaciation. *Science* 353, 470–474.
675 <https://doi.org/10.1126/science.aaf5529>
- 676 Herguera, J.C., 1992. Deep-sea benthic foraminifera and biogenic opal: Glacial to postglacial productivity
677 changes in the western equatorial Pacific. *Marine Micropaleontology, Approaches to Paleoproductivity*
678 *Reconstructions* 19, 79–98. [https://doi.org/10.1016/0377-8398\(92\)90022-C](https://doi.org/10.1016/0377-8398(92)90022-C)
- 679 Herguera, J.C., Berger, W.H., 1991. Paleoproductivity from benthic foraminifera abundance: Glacial to
680 postglacial change in the west-equatorial Pacific. *Geology* 19, 1173–1176. [https://doi.org/10.1130/0091-7613\(1991\)019<1173:PFBFAG>2.3.CO;2](https://doi.org/10.1130/0091-7613(1991)019<1173:PFBFAG>2.3.CO;2)
- 682 Hess, S., Jorissen, F.J., 2009. Distribution patterns of living benthic foraminifera from Cap Breton canyon, Bay
683 of Biscay: Faunal response to sediment instability. *Deep Sea Research Part I: Oceanographic Research Papers*
684 56, 1555–1578. <https://doi.org/10.1016/j.dsr.2009.04.003>
- 685 Hess, S., Jorissen, F.J., Venet, V., Abu-Zied, R., 2005. Benthic Foraminiferal recovery after recent turbidite
686 deposition in Cap Breton Canyon, Bay of Biscay. *Journal of Foraminiferal Research* 35, 114–129.
687 <https://doi.org/10.2113/35.2.114>
- 688 Huthnance, J.M., 1984. Slope Currents and “JEBAR.” *Journal of Physical Oceanography* 14, 795–810.
689 [https://doi.org/10.1175/1520-0485\(1984\)014<0795:SCA>2.0.CO;2](https://doi.org/10.1175/1520-0485(1984)014<0795:SCA>2.0.CO;2)
- 690 Huthnance, J.M., Inall, M.E., Fraser, N.J., 2020. Oceanic Density/Pressure Gradients and Slope Currents. *Journal*
691 *of Physical Oceanography* 50, 1643–1654. <https://doi.org/10.1175/JPO-D-19-0134.1>
- 692 Jennings, A.E., Weiner, N.J., Helgadottir, G., Andrews, J.T., 2004. Modern foraminiferal faunas of the
693 southwestern to northern Iceland Shelf: oceanographic and environmental controls. *Journal of Foraminiferal*
694 *Research* 34, 180–207. <https://doi.org/10.2113/34.3.180>
- 695 Jones, R., Brady, H., 1994. *The challenger foraminifera*, Oxford University Press, USA. ed.
- 696 Jorissen, F.J., 1999. Benthic foraminiferal microhabitats below the sediment-water interface, in: Sen Gupta, B.K.
697 (Ed.), *Modern Foraminifera*. Springer Netherlands, Dordrecht, pp. 161–179. https://doi.org/10.1007/0-306-48104-9_10
- 699 Jorissen, F.J., 1987. The distribution of benthic foraminifera in the Adriatic Sea. *Marine Micropaleontology* 12,
700 21–48. [https://doi.org/10.1016/0377-8398\(87\)90012-0](https://doi.org/10.1016/0377-8398(87)90012-0)
- 701 Jorissen, F.J., Fontanier, C., Thomas, E., 2007. Chapter Seven Paleooceanographical Proxies Based on Deep-Sea
702 Benthic Foraminiferal Assemblage Characteristics, in: Hillaire–Marcel, C., De Vernal, A. (Eds.), *Developments*
703 *in Marine Geology, Proxies in Late Cenozoic Paleooceanography*. Elsevier, pp. 263–325.
704 [https://doi.org/10.1016/S1572-5480\(07\)01012-3](https://doi.org/10.1016/S1572-5480(07)01012-3)
- 705 Jorissen, F.J., Wittling, I., Peypouquet, J.P., Rabouille, C., Relexans, J.C., 1998. Live benthic foraminiferal
706 faunas off Cape Blanc, NW-Africa: Community structure and microhabitats. *Deep Sea Research Part I:*
707 *Oceanographic Research Papers* 45, 2157–2188. [https://doi.org/10.1016/S0967-0637\(98\)00056-9](https://doi.org/10.1016/S0967-0637(98)00056-9)
- 708 Keffer, T., Martinson, D.G., Corliss, B.H., 1988. The Position of the Gulf Stream During Quaternary
709 Glaciations. *Science* 241, 440–442. <https://doi.org/10.1126/science.241.4864.440>

- 710 Keul, N., Langer, G., Thoms, S., de Nooijer, L.J., Reichart, G.-J., Bijma, J., 2017. Exploring foraminiferal Sr/Ca
711 as a new carbonate system proxy. *Geochimica et Cosmochimica Acta* 202, 374–386.
712 <https://doi.org/10.1016/j.gca.2016.11.022>
- 713 Kissel, C., Laj, C., Piotrowski, A.M., Goldstein, S.L., Hemming, S.R., 2008. Millennial-scale propagation of
714 Atlantic deep waters to the glacial Southern Ocean. *Paleoceanography* 23.
715 <https://doi.org/10.1029/2008PA001624>
- 716 Koho, K.A., Piña-Ochoa, E., Geslin, E., Risgaard-Petersen, N., 2011. Vertical migration, nitrate uptake and
717 denitrification: survival mechanisms of foraminifers (*Globobulimina turgida*) under low oxygen conditions.
718 *FEMS Microbiology Ecology* 75, 273–283. <https://doi.org/10.1111/j.1574-6941.2010.01010.x>
- 719 Korsun, S.A., Pogodina, I.A., Forman, S.L., Lubinski, D.J., 1995. Recent foraminifera in glaciomarine sediments
720 from three arctic fjords of Novaja Zemlja and Svalbard. *Polar Research* 14, 15–32.
721 <https://doi.org/10.3402/polar.v14i1.6648>
- 722 Lebreiro, S.M., Antón, L., Reguera, M.I., Marzocchi, A., 2018. Paleooceanographic and climatic implications of a
723 new Mediterranean Outflow branch in the southern Gulf of Cadiz. *Quaternary Science Reviews* 197, 92–111.
724 <https://doi.org/10.1016/j.quascirev.2018.07.036>
- 725 Löffverström, M., Caballero, R., Nilsson, J., Kleman, J., 2014. Evolution of the large-scale atmospheric
726 circulation in response to changing ice sheets over the last glacial cycle. *Climate of the Past* 10, 1453–1471.
727 <https://doi.org/10.5194/cp-10-1453-2014>
- 728 Lozier, M.S., Li, F., Bacon, S., Bahr, F., Bower, A.S., Cunningham, S.A., Jong, M.F. de, Steur, L. de, deYoung,
729 B., Fischer, J., Gary, S.F., Greenan, B.J.W., Holliday, N.P., Houk, A., Houpert, L., Inall, M.E., Johns, W.E.,
730 Johnson, H.L., Johnson, C., Karstensen, J., Komar, G., Bras, I.A.L., Lin, X., Mackay, N., Marshall, D.P.,
731 Mercier, H., Oltmanns, M., Pickart, R.S., Ramsey, A.L., Rayner, D., Straneo, F., Thierry, V., Torres, D.J.,
732 Williams, R.G., Wilson, C., Yang, J., Yashayaev, I., Zhao, J., 2019. A sea change in our view of overturning in
733 the subpolar North Atlantic. *Science* 363, 516–521. <https://doi.org/10.1126/science.aau6592>
- 734 Lynch-Stieglitz, J., 2017. The Atlantic Meridional Overturning Circulation and Abrupt Climate Change. *Annu.*
735 *Rev. Mar. Sci.* 9, 83–104. <https://doi.org/10.1146/annurev-marine-010816-060415>
- 736 Lynch-Stieglitz, J., Adkins, J.F., Curry, W.B., Dokken, T., Hall, I.R., Herguera, J.C., Hirschi, J.J.-M., Ivanova,
737 E.V., Kissel, C., Marchal, O., Marchitto, T.M., McCave, I.N., McManus, J.F., Mulitza, S., Ninnemann, U.,
738 Peeters, F., Yu, E.-F., Zahn, R., 2007. Atlantic Meridional Overturning Circulation During the Last Glacial
739 Maximum. *Science* 316, 66–69. <https://doi.org/10.1126/science.1137127>
- 740 Mackensen, A., Sejrup, H.P., Jansen, E., 1985. The distribution of living benthic foraminifera on the continental
741 slope and rise off southwest Norway. *Marine Micropaleontology* 9, 275–306. [https://doi.org/10.1016/0377-8398\(85\)90001-5](https://doi.org/10.1016/0377-8398(85)90001-5)
- 743 Marcott, S.A., Clark, P.U., Padman, L., Klinkhammer, G.P., Springer, S.R., Liu, Z., Otto-Bliesner, B.L., Carlson,
744 A.E., Ungerer, A., Padman, J., He, F., Cheng, J., Schmittner, A., 2011. Ice-shelf collapse from subsurface
745 warming as a trigger for Heinrich events. *Proc. Natl. Acad. Sci. U.S.A.* 108, 13415–13419.
746 <https://doi.org/10.1073/pnas.1104772108>
- 747 Margreth, S., Rüggeberg, A., Spezzaferri, S., 2009. Benthic foraminifera as bioindicator for cold-water coral reef
748 ecosystems along the Irish margin. *Deep Sea Research Part I: Oceanographic Research Papers* 56, 2216–2234.
749 <https://doi.org/10.1016/j.dsr.2009.07.009>
- 750 Marsh, R., Haigh, I.D., Cunningham, S.A., Inall, M.E., Porter, M., Moat, B.I., 2017. Large-scale forcing of the
751 European Slope Current and associated inflows to the North Sea. *Ocean Sci.* 13. <https://doi.org/10.5194/os-13-315-2017>
- 753 McCave, I.N., Manighetti, B., Beveridge, N. a. S., 1995. Circulation in the glacial North Atlantic inferred from
754 grain-size measurements. *Nature* 374, 149–152. <https://doi.org/10.1038/374149a0>

- 755 McManus, J.F., Francois, R., Gherardi, J.-M., Keigwin, L.D., Brown-Leger, S., 2004. Collapse and rapid
756 resumption of Atlantic meridional circulation linked to deglacial climate changes. *Nature* 428, 834–837.
757 <https://doi.org/10.1038/nature02494>
- 758 McManus, J.F., Oppo, D.W., Cullen, J.L., 1999. A 0.5-Million-Year Record of Millennial-Scale Climate
759 Variability in the North Atlantic. *Science* 283, 971–975. <https://doi.org/10.1126/science.283.5404.971>
- 760 Mendes, I., Dias, J.A., Schönfeld, J., Ferreira, Ó., 2012. Distribution of living benthic foraminifera on the
761 northern gulf of Cadiz continental shelf. *Journal of Foraminiferal Research* 42, 18–38.
762 <https://doi.org/10.2113/gsjfr.42.1.18>
- 763 Ménot, G., Bard, E., Rostek, F., Weijers, J.W.H., Hopmans, E.C., Schouten, S., Damsté, J.S.S., 2006. Early
764 Reactivation of European Rivers During the Last Deglaciation. *Science* 313, 1623–1625.
765 <https://doi.org/10.1126/science.1130511>
- 766 Milker, Y., Schmiiedl, G., 2012. A taxonomic guide to modern benthic shelf foraminifera of the western
767 Mediterranean Sea. *Palaeontol Electron* 15, 1–134. <https://doi.org/10.26879/271>
- 768 Mix, A.C., Bard, E., Schneider, R., 2001. Environmental processes of the ice age: land, oceans, glaciers
769 (EPILOG). *Quat. Sci. Rev.* 20, 627–657. [https://doi.org/10.1016/S0277-3791\(00\)00145-1](https://doi.org/10.1016/S0277-3791(00)00145-1)
- 770 Mojtahid, M., Geslin, E., Coynel, A., Gorse, L., Vella, C., Davranche, A., Zozzolo, L., Blanchet, L., Bénéteau,
771 E., Mailliet, G., 2016. Spatial distribution of living (Rose Bengal stained) benthic foraminifera in the Loire
772 estuary (western France). *Journal of Sea Research, Recent and past sedimentary, biogeochemical and benthic*
773 *ecosystem evolution of the Loire Estuary (Western France)* 118, 1–16.
774 <https://doi.org/10.1016/j.seares.2016.02.003>
- 775 Mojtahid, M., Griveaud, C., Fontanier, C., Anschutz, P., Jorissen, F.J., 2010. Live benthic foraminiferal faunas
776 along a bathymetrical transect (140–4800m) in the Bay of Biscay (NE Atlantic). *Revue de Micropaléontologie,*
777 *Foraminiferal Geobiology* 53, 139–162. <https://doi.org/10.1016/j.revmic.2010.01.002>
- 778 Mojtahid, M., Jorissen, F., Lansard, B., Fontanier, C., Bombled, B., Rabouille, C., 2009. Spatial distribution of
779 live benthic foraminifera in the Rhône prodelta: Faunal response to a continental–marine organic matter gradient.
780 *Marine Micropaleontology* 70, 177–200. <https://doi.org/10.1016/j.marmicro.2008.12.006>
- 781 Mojtahid, M., Jorissen, F.J., Garcia, J., Schiebel, R., Michel, E., Eynaud, F., Gillet, H., Cremer, M., Diz Ferreiro,
782 P., Siccha, M., Howa, H., 2013. High resolution Holocene record in the southeastern Bay of Biscay: Global
783 versus regional climate signals. *Palaeogeography, Palaeoclimatology, Palaeoecology* 377, 28–44.
784 <https://doi.org/10.1016/j.palaeo.2013.03.004>
- 785 Mojtahid, M., Toucanne, S., Fentimen, R., Barras, C., Le Houedec, S., Soulet, G., Bourillet, J.-F., Michel, E.,
786 2017. Changes in northeast Atlantic hydrology during Termination I: Insights from Celtic margin’s benthic
787 foraminifera. *Quaternary Science Reviews* 175, 45–59. <https://doi.org/10.1016/j.quascirev.2017.09.003>
- 788 Morigi, C., Jorissen, F.J., Gervais, A., Guichard, S., Borsetti, A.M., 2001. Benthic foraminiferal faunas in
789 surface sediments off nw africa: relationship with organic flux to the ocean floor. *Journal of Foraminiferal*
790 *Research* 31, 350–368. <https://doi.org/10.2113/0310350>
- 791 Moritz, M., Jochumsen, K., Kieke, D., Klein, B., Klein, H., Köllner, M., Rhein, M., 2021. Volume Transport
792 Time Series and Variability of the North Atlantic Eastern Boundary Current at Goban Spur. *Journal of*
793 *Geophysical Research: Oceans* 126, e2021JC017393. <https://doi.org/10.1029/2021JC017393>
- 794 Murray, J.W., 2014. *Ecology and Palaeoecology of Benthic Foraminifera*. Routledge.
- 795 Murray, J.W., 2006. *Ecology and Applications of Benthic Foraminifera*. Cambridge University Press.
- 796 Murray, J.W., 1970. Foraminifers of the Western Approaches to the English Channel. *Micropaleontology* 16,
797 471–485. <https://doi.org/10.2307/1485074>

- 798 Ng, H.C., Robinson, L.F., McManus, J.F., Mohamed, K.J., Jacobel, A.W., Ivanovic, R.F., Gregoire, L.J., Chen,
799 T., 2018. Coherent deglacial changes in western Atlantic Ocean circulation. *Nat Commun* 9, 2947.
800 <https://doi.org/10.1038/s41467-018-05312-3>
- 801 Otto-Bliesner, B.L., Brady, E.C., Clauzet, G., Tomas, R., Levis, S., Kothavala, Z., 2006. Last Glacial Maximum
802 and Holocene Climate in CCSM3. *Journal of Climate* 19, 2526–2544. <https://doi.org/10.1175/JCLI3748.1>
- 803 Pascual, A., Rodríguez-Lázaro, J., Martínez-García, B., Varela, Z., 2020. Palaeoceanographic and palaeoclimatic
804 changes during the last 37,000 years detected in the SE Bay of Biscay based on benthic foraminifera. *Quaternary*
805 *International*, Quaternary Research in Spain: Environmental Changes and Human Footprint 566–567, 323–336.
806 <https://doi.org/10.1016/j.quaint.2020.03.043>
- 807 Pascual, A., Rodriguez-Lazaro, J., Martín-Rubio, M., Jouanneau, J.-M., Weber, O., 2008. A survey of the
808 benthic microfauna (foraminifera, Ostracoda) on the Basque shelf, southern Bay of Biscay. *Journal of Marine*
809 *Systems*, Oceanography of the Bay of Biscay 72, 35–63. <https://doi.org/10.1016/j.jmarsys.2007.05.015>
- 810 Peck, V.L., Hall, I.R., Zahn, R., Elderfield, H., Grousset, F., Hemming, S.R., Scourse, J.D., 2006. High
811 resolution evidence for linkages between NW European ice sheet instability and Atlantic Meridional Overturning
812 Circulation. *Earth and Planetary Science Letters* 243, 476–488. <https://doi.org/10.1016/j.epsl.2005.12.023>
- 813 Peck, V.L., Hall, I.R., Zahn, R., Grousset, F., Hemming, S.R., Scourse, J.D., 2007. The relationship of Heinrich
814 events and their European precursors over the past 60ka BP: a multi-proxy ice-rafted debris provenance study in
815 the North East Atlantic. *Quaternary Science Reviews* 26, 862–875.
816 <https://doi.org/10.1016/j.quascirev.2006.12.002>
- 817 Phleger, F.B., Parker, F.L., Peirson, J.F., 1953. North Atlantic foraminifera.
- 818 Pina-Ochoa, E., Hogslund, S., Geslin, E., Cedhagen, T., Revsbech, N.P., Nielsen, L.P., Schweizer, M., Jorissen,
819 F., Rysgaard, S., Risgaard-Petersen, N., 2010. Widespread occurrence of nitrate storage and denitrification
820 among Foraminifera and Gromiida. *Proceedings of the National Academy of Sciences* 107, 1148–1153.
821 <https://doi.org/10.1073/pnas.0908440107>
- 822 Pingree, R.D., Cann, B.L., 1990. Structure, strength and seasonality of the slope currents in the Bay of Biscay
823 region. *Journal of the Marine Biological Association of the United Kingdom* 70, 857–885.
824 <https://doi.org/10.1017/S0025315400059117>
- 825 Pingree, R.D., Sinha, B., Griffiths, C.R., 1999. Seasonality of the European slope current (Goban Spur) and
826 ocean margin exchange. *Continental Shelf Research* 19, 929–975. [https://doi.org/10.1016/S0278-](https://doi.org/10.1016/S0278-4343(98)00116-2)
827 [4343\(98\)00116-2](https://doi.org/10.1016/S0278-4343(98)00116-2)
- 828 Pollard, R.T., Pu, S., 1985. Structure and circulation of the Upper Atlantic Ocean northeast of the Azores.
829 *Progress in Oceanography* 14, 443–462. [https://doi.org/10.1016/0079-6611\(85\)90022-9](https://doi.org/10.1016/0079-6611(85)90022-9)
- 830 Polyak, L., Korsun, S., Febo, L.A., Stanovoy, V., Khusid, T., Hald, M., Paulsen, B.E., Lubinski, D.J., 2002.
831 Benthic foraminiferal assemblages from the southern Kara Sea, a river-influenced Arctic marine environment.
832 *Journal of Foraminiferal Research* 32, 252–273. <https://doi.org/10.2113/32.3.252>
- 833 Pujos, M., 1976. *Ecologie des foraminifères benthiques et des thecamoebiens de la Gironde et du plateau*
834 *continental Sud-Gascogne: application à la connaissance du quaternaire terminal de la région Ouest-Gironde*
835 (Thèse de doctorat). Université Bordeaux-I, 1971-2013, France.
- 836 Rasmussen, S.O., Andersen, K.K., Svensson, A.M., Steffensen, J.P., Vinther, B.M., Clausen, H.B., Siggaard-
837 Andersen, M.-L., Johnsen, S.J., Larsen, L.B., Dahl-Jensen, D., Bigler, M., Röthlisberger, R., Fischer, H., Goto-
838 Azuma, K., Hansson, M.E., Ruth, U., 2006. A new Greenland ice core chronology for the last glacial
839 termination. *Journal of Geophysical Research: Atmospheres* 111. <https://doi.org/10.1029/2005JD006079>
- 840 Rasmussen, S.O., Bigler, M., Blockley, S.P., Blunier, T., Buchardt, S.L., Clausen, H.B., Cvijanovic, I., Dahl-
841 Jensen, D., Johnsen, S.J., Fischer, H., Gkinis, V., Guillevic, M., Hoek, W.Z., Lowe, J.J., Pedro, J.B., Popp, T.,
842 Seierstad, I.K., Steffensen, J.P., Svensson, A.M., Vallenga, P., Vinther, B.M., Walker, M.J.C., Wheatley, J.J.,
843 Winstrup, M., 2014. A stratigraphic framework for abrupt climatic changes during the Last Glacial period based
844 on three synchronized Greenland ice-core records: refining and extending the INTIMATE event stratigraphy.

- 845 Quaternary Science Reviews, Dating, Synthesis, and Interpretation of Palaeoclimatic Records and Model-data
846 Integration: Advances of the INTIMATE project (INTEgration of Ice core, Marine and TERrestrial records, COST
847 Action ES0907) 106, 14–28. <https://doi.org/10.1016/j.quascirev.2014.09.007>
- 848 Rasmussen, S.O., Seierstad, I.K., Andersen, K.K., Bigler, M., Dahl-Jensen, D., Johnsen, S.J., 2008.
849 Synchronization of the NGRIP, GRIP, and GISP2 ice cores across MIS 2 and palaeoclimatic implications.
850 Quaternary Science Reviews, INTEgration of Ice-core, Marine and Terrestrial records (INTIMATE): Refining
851 the record of the Last Glacial-Interglacial Transition 27, 18–28. <https://doi.org/10.1016/j.quascirev.2007.01.016>
- 852 Reimer, P.J., Austin, W.E.N., Bard, E., Bayliss, A., Blackwell, P.G., Ramsey, C.B., Butzin, M., Cheng, H.,
853 Edwards, R.L., Friedrich, M., Grootes, P.M., Guilderson, T.P., Hajdas, I., Heaton, T.J., Hogg, A.G., Hughen,
854 K.A., Kromer, B., Manning, S.W., Muscheler, R., Palmer, J.G., Pearson, C., Plicht, J. van der, Reimer, R.W.,
855 Richards, D.A., Scott, E.M., Southon, J.R., Turney, C.S.M., Wacker, L., Adolphi, F., Büntgen, U., Capano, M.,
856 Fahrni, S.M., Fogtmann-Schulz, A., Friedrich, R., Köhler, P., Kudsk, S., Miyake, F., Olsen, J., Reinig, F.,
857 Sakamoto, M., Sookdeo, A., Talamo, S., 2020. The IntCal20 Northern Hemisphere Radiocarbon Age Calibration
858 Curve (0–55 cal kBP). *Radiocarbon* 62, 725–757. <https://doi.org/10.1017/RDC.2020.41>
- 859 Rickaby, R.E.M., Elderfield, H., 2005. Evidence from the high-latitude North Atlantic for variations in Antarctic
860 Intermediate water flow during the last deglaciation. *Geochemistry, Geophysics, Geosystems* 6.
861 <https://doi.org/10.1029/2004GC000858>
- 862 Risgaard-Petersen, N., Langezaal, A.M., Ingvarsdén, S., Schmid, M.C., Jetten, M.S.M., Op den Camp, H.J.M.,
863 Derksen, J.W.M., Piña-Ochoa, E., Eriksson, S.P., Peter Nielsen, L., Peter Revsbech, N., Cedhagen, T., van der
864 Zwaan, G.J., 2006. Evidence for complete denitrification in a benthic foraminifer. *Nature* 443, 93–96.
865 <https://doi.org/10.1038/nature05070>
- 866 Rodriguez-Lazaro, J., Pascual, A., Cacho, I., Varela, Z., Pena, L.D., 2017. Deep-sea benthic response to rapid
867 climatic oscillations of the last glacial cycle in the SE Bay of Biscay. *Journal of Sea Research, Changing
868 Ecosystems in the Bay of Biscay: Natural and Anthropogenic Effects* 130, 49–72.
869 <https://doi.org/10.1016/j.seares.2017.06.002>
- 870 Rogerson, M., Rohling, E.J., Bigg, G.R., Ramirez, J., 2012. Paleoceanography of the Atlantic-Mediterranean
871 exchange: Overview and first quantitative assessment of climatic forcing. *Reviews of Geophysics* 50.
872 <https://doi.org/10.1029/2011RG000376>
- 873 Rühlemann, C., Mulitza, S., Lohmann, G., Paul, A., Prange, M., Wefer, G., 2004. Intermediate depth warming in
874 the tropical Atlantic related to weakened thermohaline circulation: Combining paleoclimate data and modeling
875 results for the last deglaciation. *Paleoceanography* 19. <https://doi.org/10.1029/2003PA000948>
- 876 Schmiedl, G., de Bovée, F., Buscail, R., Charrière, B., Hemleben, C., Medernach, L., Picon, P., 2000. Trophic
877 control of benthic foraminiferal abundance and microhabitat in the bathyal Gulf of Lions, western Mediterranean
878 Sea. *Marine Micropaleontology* 40, 167–188. [https://doi.org/10.1016/S0377-8398\(00\)00038-4](https://doi.org/10.1016/S0377-8398(00)00038-4)
- 879 Schmiedl, G., Mackensen, A., 1997. Late Quaternary paleoproductivity and deep water circulation in the eastern
880 South Atlantic Ocean: Evidence from benthic foraminifera. *Palaeogeography, Palaeoclimatology, Palaeoecology*
881 130, 43–80. [https://doi.org/10.1016/S0031-0182\(96\)00137-X](https://doi.org/10.1016/S0031-0182(96)00137-X)
- 882 Schmiedl, G., Mackensen, A., Müller, P.J., 1997. Recent benthic foraminifera from the eastern South Atlantic
883 Ocean: Dependence on food supply and water masses. *Marine Micropaleontology* 32, 249–287.
884 [https://doi.org/10.1016/S0377-8398\(97\)00023-6](https://doi.org/10.1016/S0377-8398(97)00023-6)
- 885 Schmiedl, G., Mitschele, A., Beck, S., Emeis, K.-C., Hemleben, C., Schulz, H., Sperling, M., Weldeab, S., 2003.
886 Benthic foraminiferal record of ecosystem variability in the eastern Mediterranean Sea during times of sapropel
887 S5 and S6 deposition. *Palaeogeography, Palaeoclimatology, Palaeoecology* 190, 139–164.
888 [https://doi.org/10.1016/S0031-0182\(02\)00603-X](https://doi.org/10.1016/S0031-0182(02)00603-X)
- 889 Schönfeld, J., 2006. Taxonomy and distribution of the *Uvigerina peregrina* plexus in the tropical to northeastern
890 Atlantic. *Journal of Foraminiferal Research* 36, 355–367. <https://doi.org/10.2113/gsjfr.36.4.355>

- 891 Schönfeld, J., 2002a. A new benthic foraminiferal proxy for near-bottom current velocities in the Gulf of Cadiz,
892 northeastern Atlantic Ocean. *Deep Sea Research Part I: Oceanographic Research Papers* 49, 1853–1875.
893 [https://doi.org/10.1016/S0967-0637\(02\)00088-2](https://doi.org/10.1016/S0967-0637(02)00088-2)
- 894 Schönfeld, J., 2002b. Recent benthic foraminiferal assemblages in deep high-energy environments from the Gulf
895 of Cadiz (Spain). *Marine Micropaleontology* 44, 141–162. [https://doi.org/10.1016/S0377-8398\(01\)00039-1](https://doi.org/10.1016/S0377-8398(01)00039-1)
- 896 Schönfeld, J., 1997. The impact of the Mediterranean Outflow Water (MOW) on benthic foraminiferal
897 assemblages and surface sediments at the southern Portuguese continental margin. *Marine Micropaleontology*
898 29, 211–236. [https://doi.org/10.1016/S0377-8398\(96\)00050-3](https://doi.org/10.1016/S0377-8398(96)00050-3)
- 899 Schönfeld, J., Altenbach, A.V., 2005. Late Glacial to Recent distribution pattern of deep-water *Uvigerina* species
900 in the north-eastern Atlantic. *Marine Micropaleontology* 57, 1–24.
901 <https://doi.org/10.1016/j.marmicro.2005.05.004>
- 902 Schroder-Adams, C., Cole, F., Medioli, F., Mudie, P., Scott, D., Dobbin, L., 1990. Recent Arctic shelf
903 Foraminifera: seasonally ice covered vs. perennially ice covered areas. *Journal of Foraminiferal Research - J*
904 *FORAMIN RES* 20, 8–36. <https://doi.org/10.2113/gsjfr.20.1.8>
- 905 Scourse, J.D., Haapaniemi, A.I., Colmenero-Hidalgo, E., Peck, V.L., Hall, I.R., Austin, W.E.N., Knutz, P.C.,
906 Zahn, R., 2009. Growth, dynamics and deglaciation of the last British–Irish ice sheet: the deep-sea ice-rafted
907 detritus record. *Quaternary Science Reviews* 28, 3066–3084. <https://doi.org/10.1016/j.quascirev.2009.08.009>
- 908 Shaffer, G., Olsen, S.M., Bjerrum, C.J., 2004. Ocean subsurface warming as a mechanism for coupling
909 Dansgaard-Oeschger climate cycles and ice-rafting events. *Geophys. Res. Lett.* 31, L24202.
910 <https://doi.org/10.1029/2004GL020968>
- 911 Spezzaferri, S., Rüggeberg, A., Stalder, C., 2015. Atlas of Benthic Foraminifera from Cold-Water Coral Reefs |
912 GeoScienceWorld Books | GeoScienceWorld. Cushman Found. Foraminifer. Res. 44.
- 913 Stern, J.V., Lisiecki, L.E., 2013. North Atlantic circulation and reservoir age changes over the past 41,000 years.
914 *Geophys. Res. Lett.* 40, 3693–3697. <https://doi.org/10.1002/grl.50679>
- 915 Thornalley, D.J.R., Bauch, H.A., Gebbie, G., Guo, W., Ziegler, M., Bernasconi, S.M., Barker, S., Skinner, L.C.,
916 Yu, J., 2015. A warm and poorly ventilated deep Arctic Mediterranean during the last glacial period. *Science*
917 349, 706–710. <https://doi.org/10.1126/science.aaa9554>
- 918 Thornalley, D.J.R., Elderfield, H., McCave, I.N., 2010. Intermediate and deep water paleoceanography of the
919 northern North Atlantic over the past 21,000 years. *Paleoceanography* 25.
920 <https://doi.org/10.1029/2009PA001833>
- 921 Toucanne, S., Naughton, F., Rodrigues, T., Vázquez-Riveiros, N., Sánchez Goñi, M.F., 2022. Chapter 25 -
922 Abrupt (or millennial or suborbital) climatic variability: Heinrich events/stadials, in: Palacios, D., Hughes, P.D.,
923 García-Ruiz, J.M., Andrés, N. (Eds.), *European Glacial Landscapes*. Elsevier, pp. 181–187.
924 <https://doi.org/10.1016/B978-0-12-823498-3.00062-5>
- 925 Toucanne, S., Soulet, G., Freslon, N., Jacinto, R.S., Dennielou, B., Zaragosi, S., Eynaud, F., Bourillet, J.-F.,
926 Bayon, G., 2015. Millennial-scale fluctuations of the European Ice Sheet at the end of the last glacial, and their
927 potential impact on global climate. *Quaternary Science Reviews* 123, 113–133.
- 928 Toucanne, S., Soulet, G., Riveiros, N.V., Boswell, S.M., Dennielou, B., Waelbroeck, C., Bayon, G., Mojtahid,
929 M., Bosq, M., Sabine, M., Zaragosi, S., Bourillet, J.-F., Mercier, H., 2021. The North Atlantic Glacial Eastern
930 Boundary Current as a Key Driver for Ice-Sheet—Amoc Interactions and Climate Instability. *Paleoceanography*
931 and *Paleoclimatology* 36, e2020PA004068. <https://doi.org/10.1029/2020PA004068>
- 932 Toucanne, S., Zaragosi, S., Bourillet, J.F., Cremer, M., Eynaud, F., Van Vliet-Lanoë, B., Penaud, A., Fontanier,
933 C., Turon, J.L., Cortijo, E., Gibbard, P.L., 2009. Timing of massive ‘Fleuve Manche’ discharges over the last
934 350kyr: insights into the European ice-sheet oscillations and the European drainage network from MIS 10 to 2.
935 *Quaternary Science Reviews* 28, 1238–1256. <https://doi.org/10.1016/j.quascirev.2009.01.006>

- 936 Toucanne, S., Zaragosi, S., Bourillet, J.-F., Dennielou, B., Jorry, S.J., Jouet, G., Cremer, M., 2012. External
937 controls on turbidite sedimentation on the glacially-influenced Armorican margin (Bay of Biscay, western
938 European margin). *Marine Geology* 303–306, 137–153. <https://doi.org/10.1016/j.margeo.2012.02.008>
- 939 Toucanne, S., Zaragosi, S., Bourillet, J.-F., Marieu, V., Cremer, M., Kageyama, M., Van Vliet-Lanoë, B.,
940 Eynaud, F., Turon, J.-L., Gibbard, P.L., 2010. The first estimation of Fleuve Manche palaeoriver discharge
941 during the last deglaciation: Evidence for Fennoscandian ice sheet meltwater flow in the English Channel ca 20–
942 18ka ago. *Earth and Planetary Science Letters* 290, 459–473. <https://doi.org/10.1016/j.epsl.2009.12.050>
- 943 Toucanne, S., Zaragosi, S., Bourillet, J.F., Naughton, F., Cremer, M., Eynaud, F., Dennielou, B., 2008. Activity
944 of the turbidite levees of the Celtic–Armorican margin (Bay of Biscay) during the last 30,000 years: Imprints of
945 the last European deglaciation and Heinrich events. *Marine Geology* 247, 84–103.
946 <https://doi.org/10.1016/j.margeo.2007.08.006>
- 947 van Aken, H.M., 2000. The hydrography of the mid-latitude Northeast Atlantic Ocean: II: The intermediate
948 water masses. *Deep Sea Research Part I: Oceanographic Research Papers* 47, 789–824.
949 [https://doi.org/10.1016/S0967-0637\(99\)00112-0](https://doi.org/10.1016/S0967-0637(99)00112-0)
- 950 Van der Zwaan, G.J., Jorissen, F.J., 1991. Biofacial patterns in river-induced shelf anoxia. *Geological Society,*
951 *London, Special Publications* 58, 65–82. <https://doi.org/10.1144/GSL.SP.1991.058.01.05>
- 952 Vénec-Peyré, M.-T., Le Calvez, Y., 1988. Les Foraminifères épiphytes de l’herbier de Posidonies de Banyuls-
953 sur-Mer (Méditerranée occidentale): étude des variations spatio-temporelles du peuplement. *Cah. micropaléontol*
954 *3*, 21–40.
- 955 Waelbroeck, C., Lougheed, B.C., Vazquez Riveiros, N., Missiaen, L., Pedro, J., Dokken, T., Hajdas, I., Wacker,
956 L., Abbott, P., Dumoulin, J.-P., Thil, F., Eynaud, F., Rossignol, L., Fersi, W., Albuquerque, A.L., Arz, H.,
957 Austin, W.E.N., Came, R., Carlson, A.E., Collins, J.A., Dennielou, B., Desprat, S., Dickson, A., Elliot, M.,
958 Farmer, C., Giraudeau, J., Gottschalk, J., Henderiks, J., Hughen, K., Jung, S., Knutz, P., Lebreiro, S., Lund,
959 D.C., Lynch-Stieglitz, J., Malaizé, B., Marchitto, T., Martínez-Méndez, G., Mollenhauer, G., Naughton, F.,
960 Nave, S., Nürnberg, D., Oppo, D., Peck, V., Peeters, F.J.C., Penaud, A., Portilho-Ramos, R. da C., Repschläger,
961 J., Roberts, J., Rühlemann, C., Salgueiro, E., Sanchez Goni, M.F., Schönfeld, J., Scussolini, P., Skinner, L.C.,
962 Skonieczny, C., Thornalley, D., Toucanne, S., Rooij, D.V., Vidal, L., Voelker, A.H.L., Wary, M., Weldeab, S.,
963 Ziegler, M., 2019. Consistently dated Atlantic sediment cores over the last 40 thousand years. *Sci Data* 6, 165.
964 <https://doi.org/10.1038/s41597-019-0173-8>
- 965 Wang, Y.J., Cheng, H., Edwards, R.L., An, Z.S., Wu, J.Y., Shen, C.-C., Dorale, J.A., 2001. A High-Resolution
966 Absolute-Dated Late Pleistocene Monsoon Record from Hulu Cave, China. *Science* 294, 2345–2348.
967 <https://doi.org/10.1126/science.1064618>
- 968 Wollenburg, J.E., Knies, J., Mackensen, A., 2004. High-resolution paleoproductivity fluctuations during the past
969 24 kyr as indicated by benthic foraminifera in the marginal Arctic Ocean. *Palaeogeography, Palaeoclimatology,*
970 *Palaeoecology* 204, 209–238. [https://doi.org/10.1016/S0031-0182\(03\)00726-0](https://doi.org/10.1016/S0031-0182(03)00726-0)
- 971 Wollenburg, J.E., Kuhnt, W., 2000. The response of benthic foraminifera to carbon flux and primary production
972 in the Arctic Ocean. *Marine Micropaleontology* 40, 189–231. [https://doi.org/10.1016/S0377-8398\(00\)00039-6](https://doi.org/10.1016/S0377-8398(00)00039-6)
- 973 Wollenburg, J.E., Kuhnt, W., Mackensen, A., 2001. Changes in Arctic Ocean paleoproductivity and
974 hydrography during the last 145 kyr: The benthic foraminiferal record. *Paleoceanography* 16, 65–77.
975 <https://doi.org/10.1029/1999PA000454>
- 976 Wollenburg, J.E., Mackensen, A., 2009. The ecology and distribution of benthic foraminifera at the Håkon
977 Mosby mud volcano (SW Barents Sea slope). *Deep Sea Research Part I: Oceanographic Research Papers* 56,
978 1336–1370. <https://doi.org/10.1016/j.dsr.2009.02.004>
- 979 Wollenburg, J.E., Mackensen, A., 1998. Living benthic foraminifera from the central Arctic Ocean: faunal
980 composition, standing stock and diversity. *Marine Micropaleontology* 34, 153–185.
981 [https://doi.org/10.1016/S0377-8398\(98\)00007-3](https://doi.org/10.1016/S0377-8398(98)00007-3)

- 982 Yu, J., Elderfield, H., Jin, Z., Tomascak, P., Rohling, E.J., 2014. Controls on Sr/Ca in benthic foraminifera and
983 implications for seawater Sr/Ca during the late Pleistocene. *Quaternary Science Reviews* 98, 1–6.
984 <https://doi.org/10.1016/j.quascirev.2014.05.018>
- 985 Zahn, R., Schönfeld, J., Kudrass, H.-R., Park, M.-H., Erlenkeuser, H., Grootes, P., 1997. Thermohaline
986 instability in the North Atlantic during meltwater events: Stable isotope and ice-rafted detritus records from Core
987 SO75-26KL, Portuguese Margin. *Paleoceanography* 12, 696–710. <https://doi.org/10.1029/97PA00581>
- 988 Zaragosi, S., Bourillet, J.-F., Eynaud, F., Toucanne, S., Denhard, B., Van Toer, A., Lanfumeu, V., 2006. The
989 impact of the last European deglaciation on the deep-sea turbidite systems of the Celtic-Armorican margin (Bay
990 of Biscay). *Geo-Mar Lett* 26, 317–329. <https://doi.org/10.1007/s00367-006-0048-9>
- 991 Zaragosi, S., Eynaud, F., Pujol, C., Auffret, G.A., Turon, J.-L., Garlan, T., 2001. Initiation of the European
992 deglaciation as recorded in the northwestern Bay of Biscay slope environments (Meriadzek Terrace and
993 Trevelyan Escarpment): a multi-proxy approach. *Earth and Planetary Science Letters* 188, 493–507.
994 [https://doi.org/10.1016/S0012-821X\(01\)00332-6](https://doi.org/10.1016/S0012-821X(01)00332-6)
- 995 Zou, S., Lozier, S., Zenk, W., Bower, A., Johns, W., 2017. Observed and modeled pathways of the Iceland
996 Scotland Overflow Water in the eastern North Atlantic. *Progress in Oceanography* 159, 211–222.
997 <https://doi.org/10.1016/j.pocean.2017.10.003>
- 998
- 999

1000 **Table 1.** ^{14}C dates of core BOBGEO-CS05.

Core label	Depth (cm)	Lab. Number ^a	Species	^{14}C age (yr BP)	error (1 σ)	Reservoir correction ^b (^{14}C yr)	error ^b (1 σ)	^{14}C age corrected for reservoir ^c (^{14}C yr BP)	error ^d (1 σ)	Calendar age range ^e (yr BP, 2 σ)
BOBGEO-CS05	0	Poz-73846	<i>N. pachyderma</i>	14100	80	970	200	13130	215	15133-16357
BOBGEO-CS05	10	Poz-42911	bulk planktonic	14770	70	970	200	13800	212	16132-17333
BOBGEO-CS05	305-309	Beta-478193	<i>G. bulloides</i>	15270	40	400	200	14870	204	17550-18661
BOBGEO-CS05	446	SacA-29355	bulk planktonic	18090	60	400	200	17690	209	20890-22026
BOBGEO-CS05	500-505	Beta-478194	<i>G. bulloides</i>	17140	50	400	200	16740	206	19773-20716
BOBGEO-CS05	660	SacA-29356	bulk planktonic	21140	200	400	200	20740	283	24238-25672
BOBGEO-CS05	796-800	Beta-478195	<i>G. bulloides</i>	19680	60	400	200	19280	209	22885-23789
BOBGEO-CS05	933-935	Beta-478196	<i>G. bulloides</i>	20430	70	400	200	20030	212	23727-24665
BOBGEO-CS05	1030-1033	Beta-478197	<i>G. bulloides</i>	21830	70	400	200	21430	212	25220-26049
BOBGEO-CS05	1230	Poz-45912	bulk planktonic	24510	240	400	200	24110	312	27726-28959
BOBGEO-CS05	1350	SacA-29357	bulk planktonic	24220	100	400	200	23820	224	27624-28628
BOBGEO-CS05	1460	Poz-73848	<i>N. pachyderma</i>	26130	230	400	200	25730	305	29237-30490

a: Poz- (Poznan Radiocarbon Lab., Poland); Beta- (Beta Analytic, USA); SacA- (SMA Artemis, France)

b: Reservoir correction inferred from Stern et Lisieki (2013); see Toucanne et al. (2015) for details

c: Corrected ^{14}C ages are obtained by subtracting the reservoir correction to the original ^{14}C age

d: Errors associated to the corrected ^{14}C were propagated through the quadratic sum

e: Corrected ^{14}C ages were calibrated using the atmospheric calibration curve IntCal20 (Reimer et al., 2020)

1001

1002

1003

1004 **Table 2.** Taxonomic reference list, microhabitat and ecological preferences for the dominant
 1005 benthic species (>5 %) and the corresponding bibliographic references.

Species	References with images	Microhabitat	Ecological preferences	Plate 1	Plate 2
<i>Bolivina</i> spp.		Shallow infaunal (Murray, 2006)	<i>Bolivina</i> spp. have opportunistic behaviour (Schmiedl <i>et al.</i> , 2000) and ecological preferences for phytodetritus enriched deposits (Duros <i>et al.</i> , 2017, 2011)	5-6	
<i>Cassidulina carinata</i> Silvestri, 1896	Phleger <i>et al.</i> (1953), pl. 9, Figs. 32–37	Epifaunal to shallow infaunal (Jorissen, 1987; Altenbach <i>et al.</i> , 1999)	<i>Cassidulina carinata</i> is an opportunistic species (Fontanier <i>et al.</i> , 2003; Duros <i>et al.</i> , 2011) that lives in OM-enriched sediments (Hess <i>et al.</i> , 2005; Hess and Jorissen, 2009).	7	
<i>Cassidulina crassa</i> d'Orbigny, 1839	Jorissen (1987), pl. 1, Fig. 3	Shallow infaunal (de Stigter <i>et al.</i> , 1998; Fontanier <i>et al.</i> , 2005)	In our case, <i>Cassidulina crassa</i> could be a morphospecies of <i>Cassidulina reniforme</i> . This latter is often transported from the continental shelf, and redeposited on glacial marine sediments (Mackensen <i>et al.</i> , 1985), until 1000m water depth in Arctic (Wollenburg and Mackensen, 2009).	8	
<i>Cibicides lobatulus</i> Walker and Jacob, 1798	Jones and Brady (1994), pl. 93, Fig. 1	Epifaunal (Murray, 2006)	<i>Cibicides lobatulus</i> live at shallow depth, attached on seagrass and algae (Véneç-Peyré and Le Calvez, 1988; Murray, 2006). Even if, they were described as transported species, they can be found alive in deep and high energy environments (e.g. Schönfeld, 1997, 2002b, 2002a; Margreth <i>et al.</i> , 2009; Spezzaferri <i>et al.</i> , 2015)	13	
<i>Cibicidoides pachyderma</i> Rzehak, 1886	Jones and Brady (1994), pl. 94, Fig. 9	Shallow infaunal (Fontanier <i>et al.</i> , 2003, 2002)	<i>Cibicidoides pachyderma</i> live in meso-oligotrophic conditions (Fontanier <i>et al.</i> , 2003; Mojtahid <i>et al.</i> , 2009). They prefer low nutrients waters (Schmiedl <i>et al.</i> , 2000).	11-12	b
<i>Chilostomella oolina</i> Schwager, 1878	Jones and Brady (1994), pl. 55, Fig. 12-14	Deep Infaunal (Corliss and Emerson, 1990; Bernhard, 1992; Jorissen <i>et al.</i> , 1998)	<i>Chilostomella oolina</i> is adapted to anoxic or suboxic conditions (Fontanier <i>et al.</i> , 2002; Bernhard and Sen Gupta, 2003). They may be replaced by <i>Globobulimina</i> spp. when the degraded OM quality decreases (Fontanier <i>et al.</i> , 2002)	4	
<i>Elphidium clavatum</i> Cushman, 1930	Darling <i>et al.</i> (2016), Fig. 4, S4	Infaunal–epifaunal (Murray, 2006)	<i>Elphidium clavatum</i> is a widespread taxon, mainly distributed in the Arctic, and frequent in glacier-proximal environments. It is found living down to several hundreds of meters depths in the Arctic and in the Baltic (Jennings <i>et al.</i> , 2004; Murray, 2006; Darling <i>et al.</i> , 2016; Fossile <i>et al.</i> , 2020). In the nearby study of Mojtahid <i>et al.</i> (2017), <i>Elphidium</i> species found at 1000 m depth during the last deglaciation were interpreted as being possibly transported from shallower settings.	10	a
<i>Elphidium gerthi</i> van Voorthuysen, 1957	Mendes <i>et al.</i> (2012), Fig. 4, 8		<i>Elphidium gerthi</i> is a subtidal to intertidal species, very common along the western European coasts. In the nearby study of Mojtahid <i>et al.</i> (2017), <i>Elphidium</i> species found at 1000 m depth during the last deglaciation were interpreted as being possibly transported from shallower settings.	9	
<i>Globobulimina</i> spp.		Deep infaunal (Murray, 2006)	<i>Globobulimina</i> spp. live in organically-enriched and/or oxygen-depleted sediments (e.g. Jorissen, 1999; Schmiedl <i>et al.</i> , 2003; Mojtahid <i>et al.</i> , 2010). They can live in anoxic sediments by respiring nitrates (Risgaard-Petersen <i>et al.</i> , 2006).	3	
<i>Gavelinopsis praegeri</i> Heron-Allen & Earland, 1913	Jorissen (1987), pl. 3, Fig. 13	Epifaunal (Jorissen, 1987)	<i>Gavelinopsis praegeri</i> is an epiphytic species living in a wide range of water depths in marine environments (Murray, 2006). They are found down to 1200m water depth (de Stigter, 1996) and prefers more oxic conditions (Dorst <i>et al.</i> , 2015).	16	

<i>Hoeglundina elegans</i> d'Orbigny, 1826	Milker and Schmiedl, (2012), pl. 19, Fig. 15	Epifaunal; shallow infaunal (Jorissen <i>et al.</i> , 1998; Fontanier <i>et al.</i> , 2002)	<i>Hoeglundina elegans</i> is described as indicator of low organic carbon environments (Fontanier <i>et al.</i> , 2002; Morigi <i>et al.</i> , 2001).	17	
<i>Nonionella turgida</i> Williamson, 1858	Milker and Schmiedl, (2012), pl. 26, Figs. 1-5	Deep infaunal (Corliss, 1991)	<i>Nonionella turgida</i> is an opportunistic species, tolerant to low oxygen conditions and high nutrient level (Van der Zwaan and Jorissen, 1991).	2	
<i>Planorbulina mediterraneensis</i> d'Orbigny, 1826	Jones and Brady (1994), pl. 92, Fig. 1	Epifaunal (Murray, 2006)	<i>Planorbulina mediterraneensis</i> is an epiphytic species and lives at shallow depths (Murray, 2006).	15	
<i>Pullenia quinqueloba</i> Reuss, 1851	Jones and Brady (1994), pl. 84, Fig. 14	Intermediate infaunal (Corliss, 1991; Fontanier <i>et al.</i> , 2008)	<i>Pullenia quinqueloba</i> can live in low-organic carbon conditions (Gupta, 1999).	18	
<i>Textularia sagittula</i> Defrance, 1824	Jorissen (1987), pl. 3, Fig. 12	Epifaunal (Murray, 2006)	<i>Textularia sagittula</i> is an agglutinated species (Murray, 2006). They are dominant in shallow water depths, on sandy sediments (Murray, 2014)	1	
<i>Trifarina angulosa</i> Williamson, 1858	Jones and Brady (1994), pl. 74, Fig. 15	Shallow infaunal (Hess and Jorissen, 2009)	<i>Trifarina angulosa</i> have been observed in phytodetritus-enriched sediment (e.g. Hess and Jorissen, 2009; Duros <i>et al.</i> , 2011). They are often associated with <i>C. lobatulus</i> to strong bottom currents and can be observed until 1000m water depth (Mackensen <i>et al.</i> , 1985).	14	

1006

1007 **9. Table caption**

1008 **Table 1.** ^{14}C dates of core BOBGEO-CS05

1009 **Table 2.** Taxonomic reference list, microhabitat and ecological preferences for the dominant
1010 benthic species (>5 %) and the corresponding bibliographic references.

1011

1012 **10. Figures Caption**

1013 **Figure 1.** Location of the study area. a) 3D representation (N-S, W-E and in water depth) of
1014 the modern oceanic circulation in the North Atlantic representing the main currents (acronyms
1015 written in black), water masses (acronyms written in colors) and the Subpolar (in blue) and
1016 Subtropical (in red) gyres in the North Atlantic. b) Bathymetric map representing the
1017 paleogeographic and paleoceanographic configuration (i.e. ice sheets, the Channel River,
1018 currents, and water masses) of the North Atlantic during the Last Glacial Stadials according to
1019 Toucanne *et al.* (2021). The angulous shapes represent the icebergs. c) Bathymetric map
1020 focussing on the study area and showing the location of our study core BOBGEO-CS05 (violet
1021 star), together with nearby cores at 1000 m water depth (black stars): MD95-2002 (Eynaud *et*
1022 *al.*, 2012; Ménot *et al.*, 2006; Toucanne *et al.*, 2015), MD99-2328 (Mojtahid *et al.*, 2017), PP10-
1023 12 (Pascual *et al.*, 2020). For the detailed description of the general modern and glacial
1024 circulation in the North Atlantic and in the study area, the reader is referred to the text (Section
1025 2). LGM: Last Glacial Maximum.

1026

1027 **Figure 2.** Age model of core BOBGEO-CS05. a) Chronostratigraphic framework of core
1028 BOBGEO-CS05 based on the synchronisation of XRF-Ca/Ti ratios with cores MD95-2002 and
1029 MD99-2328 (Zaragosi *et al.*, 2006; Mojtahid *et al.*, 2017; Toucanne *et al.*, 2021). b) Sediment
1030 Accumulation Rate (SAR; full line) and ^{14}C dates (orange triangles) with associated errors in
1031 core BOBGEO-CS05. The ^{14}C dates represented by empty triangles are outliers (cf. section 3.1.
1032 for further details). In red is represented the final age model based on XRF-Ca/Ti
1033 synchronisation (cf. Fig. 2a). c) Test of the robustness of the age model with the percentages of
1034 the polar planktonic species *N. pachyderma* in core BOBGEO-CS05 (this study) with core
1035 MD95-2002 (Grousset *et al.*, 2000) and MD99-2328 (Mojtahid *et al.*, 2017). d) NGRIP $\delta^{18}\text{O}$
1036 (GICCS05 chronology; Rasmussen *et al.*, 2006, 2014). f) X-Ray photographs (cf.
1037 Supplementary material S1 for the whole core) showing the four observed facies. Blue triangles:

1038 ^{14}C dates of core MD95-2002 (Toucanne *et al.*, 2021); Orange and empty triangles: ^{14}C dates
1039 of core BOBGEO-CS05; Blue bands: Heinrich Stadials (HSs); Gray bands: Heinrich Events
1040 (HEs); Greenland Interstadial (GI); Last Glacial Maximum (LGM); Marine Isotope Stage
1041 (MIS).

1042

1043 **Figure 3.** Benthic foraminiferal data from core BOBGEO-CS05. a) Benthic Foraminiferal
1044 Accumulation Rates (BFAR; $\text{ind.cm}^{-3}.\text{ka}^{-1}$) for the $>150\ \mu\text{m}$ (full line) and the $>63\ \mu\text{m}$ fraction
1045 (dashed line). b) Shannon index (H). c-j) Relative abundances (%) of the eight most
1046 representative benthic foraminiferal species ($>10\%$). Full lines and dashed lines represent
1047 respectively the $>150\ \mu\text{m}$ and $>63\ \mu\text{m}$ fractions. Brown lines represent data from the $>150\ \mu\text{m}$
1048 fraction of core MD99-2328 (Mojtahid *et al.*, 2017). Yellow bands: Greenland Interstadials
1049 (GI); gray bands: Heinrich Events (HEs); blue bands: Heinrich Stadial (HSs). Marine Isotope
1050 Stage (MIS). The vertical dashed grey line represents the limit between early HS1 (ca. 18.2 -
1051 16.7 cal ka BP) and late HS1 (ca. 16.7 – 14.7 cal ka BP). To better highlight the variations of
1052 the different species groups, the scale of the ordinate axis is not constant.

1053

1054 **Figure 4:** Benthic foraminiferal response to ice-sheet/AMOC dynamics. a) Relative abundance
1055 of *N. pachyderma* in core BOBGEO-CS05. b) Relative abundances of glacier-proximal
1056 indicator species (% *Elphidium excavatum* f. *clavatum* + % *C. crassa*) in core BOBGEO-CS05.
1057 c) BIT-index at site MD95-2002 as a proxy for continental-derived material input (Ménot *et al.*,
1058 2006). d) Relative abundances of high-organic flux indicator species (% *C. carinata* + %
1059 *Bolivina* spp.) in core BOBGEO-CS05. e) Bermuda Rise $^{231}\text{Pa}/^{230}\text{Th}$ compilation as a proxy for
1060 AMOC export at $>2000\ \text{m}$ depth (McManus *et al.*, 2004; Böhm *et al.*, 2015; Henry *et al.*, 2016).
1061 f) XRF-Zr/Rb (violet line) and \overline{SS} (pink line) composite records from the northeast Atlantic
1062 including BOBGEO-CS05 as proxies for the reconstruction of GEBC flow speed changes
1063 (Toucanne *et al.*, 2021). g) Relative abundances of high-energy indicator species (% *C.*
1064 *lobatulus* + % *T. angulosa*) in core BOBGEO-CS05. h) Relative abundances of meso-
1065 oligotrophic indicator species (% *C. pachyderma*) in core BOBGEO-CS05. i) Relative
1066 abundances of anoxia indicator species (% *Globobulimina* spp. + % *C. oolina*). To better
1067 highlight the variations of the different species groups, the scale of the ordinate axis is not
1068 constant. The main events and climatic phases are reported similarly to Fig. 3.

1069

1070 **Figure 5.** Focus on HS2. a) Relative abundances of the planktonic species *N. pachyderma* in
1071 core BOBGEO-CS05 (black line; this study) and MD95-2002 (blue line; Grousset *et al.*, 2000).
1072 b) XRF-Zr/Rb (violet line) and \overline{SS} (pink line) composite records from the northeast Atlantic
1073 (including BOBGEO-CS05) as proxies for the reconstruction of GEBC flow speed changes
1074 (Toucanne *et al.*, 2021). c) Relative abundances of high-energy indicator species (% *C.*
1075 *lobatulus* + % *T. angulosa*) in core BOBGEO-CS05. d) Benthic Foraminiferal Accumulation
1076 Rates (BFAR; ind.cm⁻³.ka⁻¹) for the >150 μm in core BOBGEO-CS05. e) Relative abundances
1077 of meso-oligotrophic indicator species (% *C. pachyderma*) in core BOBGEO-CS05. f) Relative
1078 abundances of anoxia indicator species (% *Globobulimina* spp. + % *C. oolina*) in core
1079 BOBGEO-CS05. Dashed vertical line: Heinrich Event 2 (HE2) sensu stricto according to the
1080 regional Ca/Ti synchronisation (cf. Table S2 in Toucanne *et al.*, 2021); blue bands: the HS2a,b
1081 cold events (Bard *et al.*, 2000); yellow band: the mid-HS2 re-ventilation event. To better
1082 highlight the variations of the different species groups, the scale of the ordinate axis is not
1083 constant.

1084

1085 **11. Plates caption**

1086 **Plate 1.** SEM photographs of the dominant benthic species (>5 % in at least one sample): 1)
1087 *Textularia sagittula* ; 2) *Nonionella turgida* ; 3) *Globobulimina affinis* ; 4) *Chilostomella oolina*
1088 ; 5) *Bolivina subaenariensis*; 6) *Bolivina albatrossi*; 7) *Cassidulina carinata*; 8) *Cassidulina*
1089 *crassa*; 9) *Elphidium gerthi* ; 10) *Elphidium excavatum* f. *clavatum* ; 11) *Cibicidoides*
1090 *pachyderma* ; 12) *Cibicides lobatulus*; 13) *Trifarina angulosa*; 14) *Planorbulina*
1091 *mediterraneensis*; 15) *Gavelinopsis praegeri* ; 16) *Hoeglundina elegans* ; 17) *Pullenia*
1092 *quinteloba*. Scale bar = 100μm.

1093

1094 **Plate 2.** a) Natural light photographs of *Elphidium excavatum* f. *clavatum* showing pyritised
1095 and altered shells. b) SEM photographs showing the variability of the morphotypes (in lateral
1096 view) lumped into *Cibicidoides pachyderma* in this study.

1097

1098 **12. Supplementary material caption**

1099 **S1.** X-Ray radiographs of core BOBGEO-CS05

1100 **S2.** Figure representing the relative abundances of taxa present between 5 and 10 % in at least
1101 one sample

1102 **S3.** Raw foraminiferal counts

Figure 1

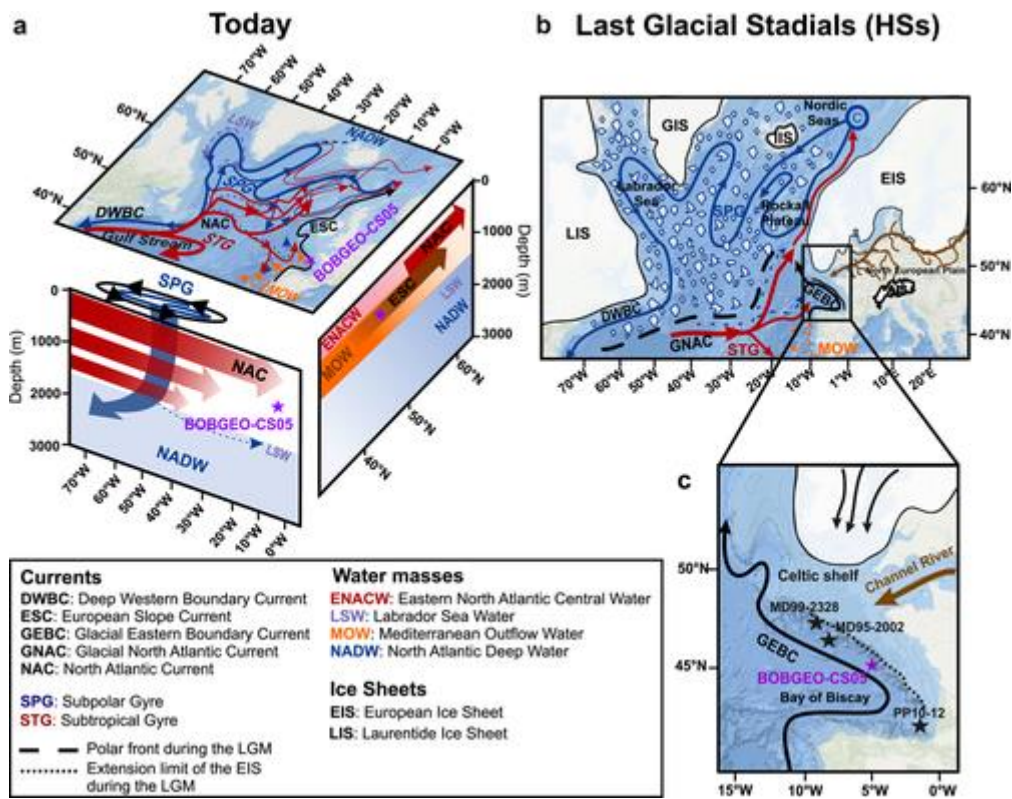


Figure 2

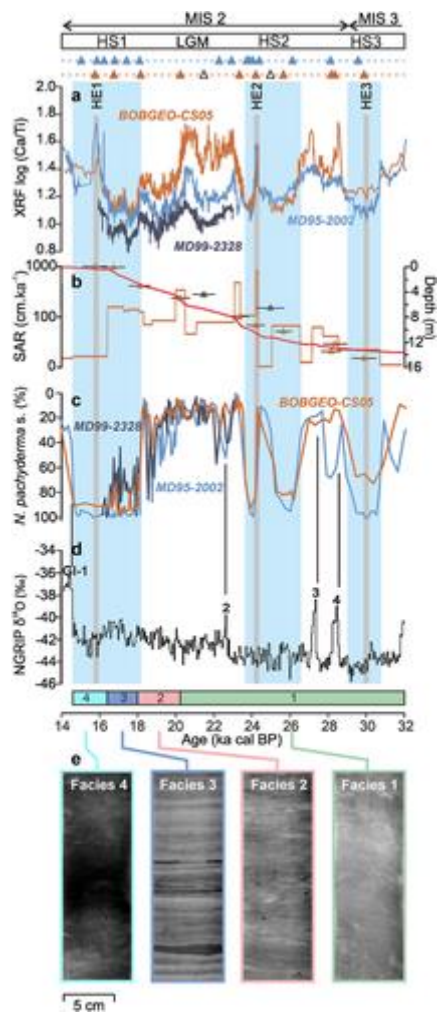


Figure 3

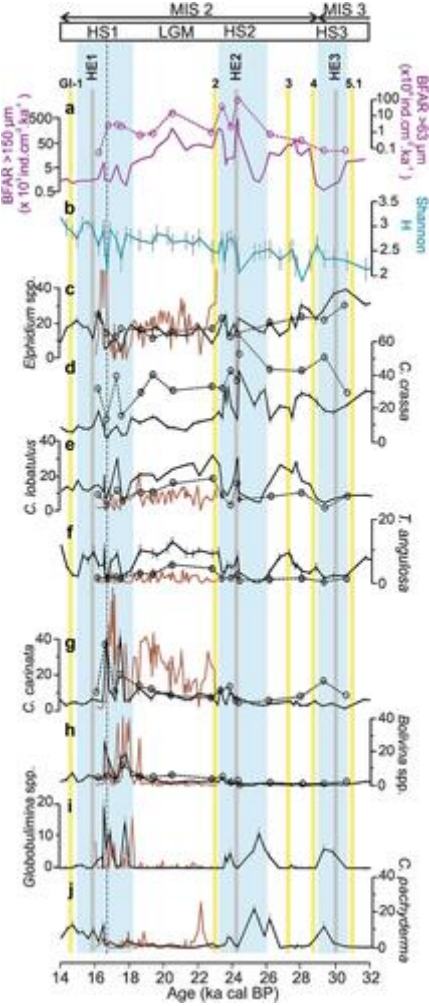


Figure 4

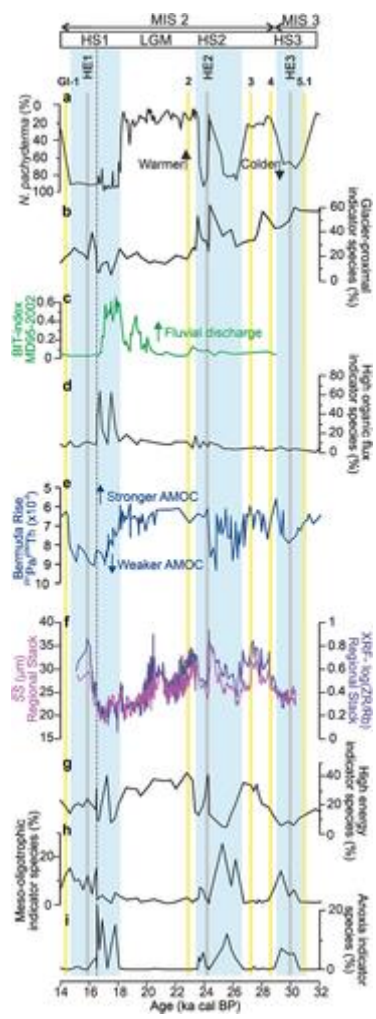


Figure 5

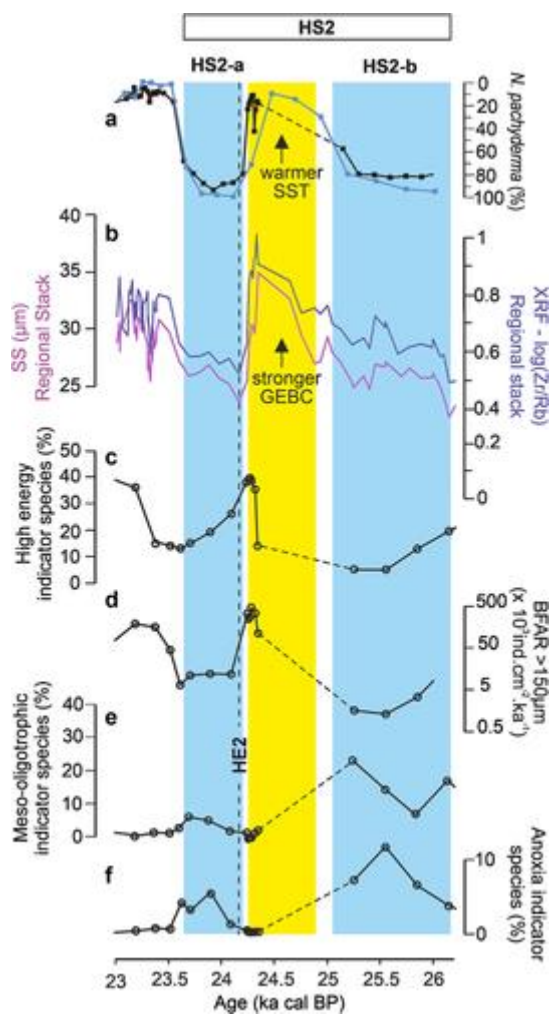


Plate 1

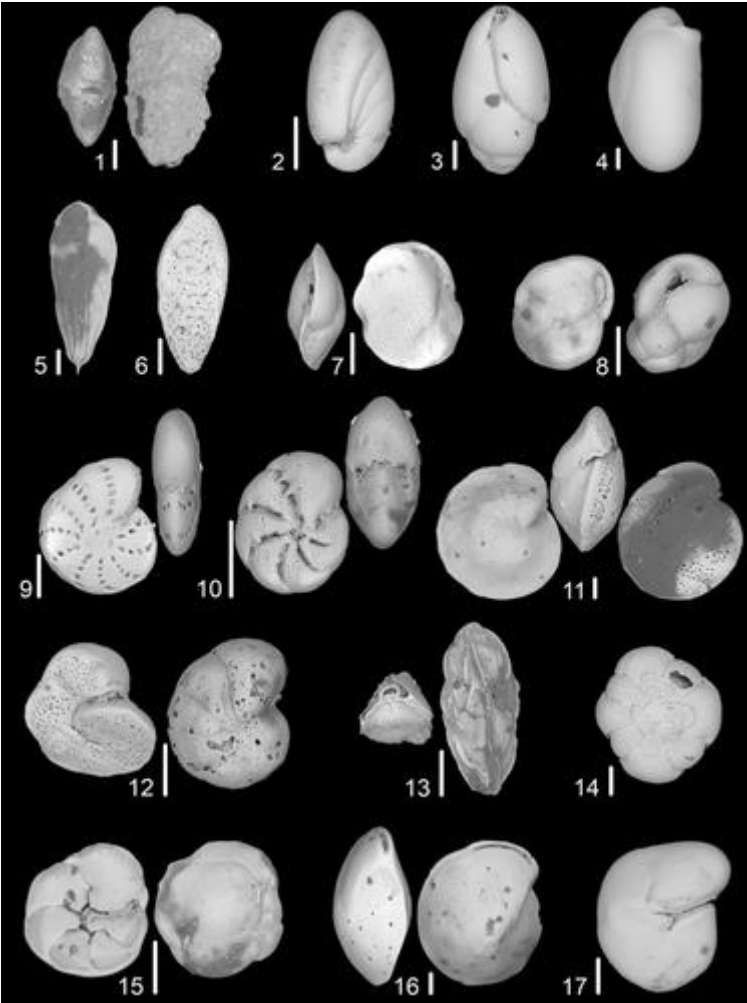
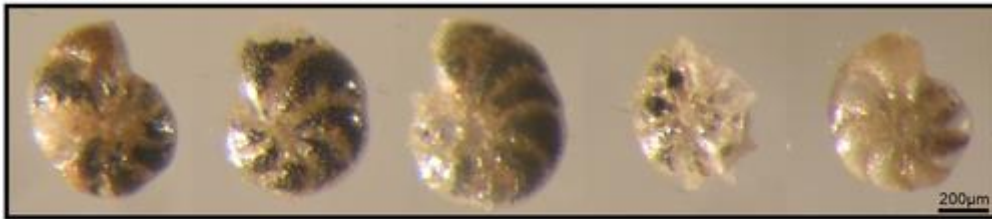


Plate 2

a *Elphidium excavatum* cf. *clavatum*



b Morphotypes of *C. pachyderma*

